Pain Rating

First, we compared pain ratings among the control (IES) and 11 IES + TS conditions to examine whether and how the conditioning tactile stimuli affect the intensity of the perceived pain sensation. The stimuli of twelve conditions were presented randomly at an interval of ~5 s and subjects assessed the intensity of the pain of each stimulus based on VAS (0–100). Ten trials were performed for each condition and the mean value was used for the analysis.

MEG Recording and Analysis

Because of the long experiment time, the MEG experiment was separated into two sessions. IES + TS conditions with CTIs of –40 to 500 ms were examined in the first session, and IES + TS conditions with CTIs of –500 to –60 ms in the second session. Therefore, there were nine conditions in the first session: control IES, control TS and seven IES + TS conditions with CTIs of –40, –20, 0, 50, 100, 300 and 500 ms. In the second session, there were six conditions: control IES, control TS and four IES + TS conditions with CTIs of –500, –300, –100 and –60 ms. The two sessions were performed on different days. Somatosensory evoked magnetic fields (SEFs) were recorded using a dual 37-channel axial-type first-order biomagnetometer (Magnes, Biomagnetic Technologies, San Diego, CA) as described previously (Kakigi et al., 2000). The probes were centered on the C3 and C4 positions as based on the International 10/20 System. The SEFs were recorded with a filter of 0.1–200 Hz at a sampling rate of 1048 Hz, and then filtered offline with a bandpass of 0.5–150 Hz. Sweeps were triggered by the conditioning stimulus (TS) in the first session and by the test stimulus (IES) in the second session. The window of analysis was from 150 ms before to 800 ms after the conditioning stimulus, and the prestimulus period was used as the DC baseline. The stimuli of various conditions were presented randomly at an interval of 3–5 s. For each condition, 50 artifact-free trials were collected. Throughout the MEG experiment, subjects were instructed to look at a fixation point presented 1m in front of them.

Since magnetic fields recorded in the IES +TS conditions were a mixture of TS- and IES-evoked responses, we subtracted the control TS-induced response from the response recorded in the IES + TS conditions to obtain the actual IES-evoked response. Then we calculated the root mean square (RMS) across all 74 channels of the subtracted waveform to compare the amplitude of the IES-evoked response among conditions. This method is easy to perform and the results are easy to understand. This method is based on the assumption that the TS-evoked response is not influenced by concomitant IES. However, in some IES + TS conditions, the TS-evoked cortical response was substantially affected by a preceding IES as will be described below. Therefore, we then calculated how the TS- and IES-evoked responses explain the waveforms of the IES + TS conditions using a least squares fit. Since the waveform for a IES + TS condition is the sum of the waveforms of IES and TS with various ratios, it can be expressed as

$$f(\text{IES}+\text{TS}) = a \times f(\text{TS}) + b \times f(\text{IES}), \quad 0 \le a, b \le 1$$

where a and b are coefficients for TS and IES, respectively. The values of a and b indicate to what extent TS and IES contribute to the activity in the IES + TS conditions. When a is much larger than b, TS contributes to the waveform much more than IES, and vice versa. To obtain the best explanation of f(IES + TS), coefficients a and b must minimize the sum difference square,

$$\sum_{i=1}^{74} (\text{IES}+\text{TS}_i - a\text{TS}_i - b\text{IES}_i)^2$$

where IES + TS$_i$ are values for an IES + TS condition, TS$_i$ are values for TS, and IES$_i$ are values for IES. For example, by applying data at a latency point of 110 ms (peak latency) after TS for the IES + TS –40 ms condition in Figure 7, we obtained the following formula and calculated a and b to minimize its number:

$$1295212a^2 + 1080948b^2 - 2249122a - 1779640b + 2045030ab + 1060634$$

By solving this problem, we get $a = 0.86$ and $b = 0.007$, which indicate that the IES-evoked response does not contribute to the waveform of

the IES + TS –40 ms condition at this latency point. By using this method, we could assess whether and how the control IES-evoked responses were changed in IES + TS conditions without being affected by changes of the conditioning stimulus-evoked response.

Data were expressed as the mean ± standard deviation. Differences of values among conditions were assessed with a one-way analysis of variance (ANOVA). P values of < 0.05 were considered significant.

Results

Pain rating

The mean pain rating for the control condition (IES alone) was 44.3 ± 9.3. The respective values for 11 paired stimuli conditions (IES + TS) with CTIs of –500, –300, –100, –60, –40, –20, 0, 50, 100, 300 and 500 ms were 43.1 ± 7.7, 42.5 ± 8.2, 39.7 ± 8.5, 37.4 ± 9.5, 12.7 ± 7.2, 11.1 ± 6.3, 13.7 ± 6.8, 16.8 ± 7.9, 23.6 ± 9.0, 29.1 ± 11.3 and 33.4 ± 13.9. Therefore, the pain rating was highest for the control condition and lowest for the IES + TS –20 ms condition. The difference among the twelve conditions was significant [$F(1,11) = 18.3$, $P < 0.0001$].

MEG Experiment

The mean onset latency of TS-induced magnetic fields (control TS) was 51.4 ± 7.2 ms for the first session and 49.2 ± 6.2 ms for the second session. The mean onset latency of IES-induced magnetic fields was 89.5 ± 15.4 ms for the first session and 87.5 ± 10.6 ms for the second session. The mean difference in onset latency between TS and IES was 38.1 ms (ranging from 16.2 to 59.5 ms) for the first session and 38.3 ms (from 18.2 to 54.8) in the second session. In all subjects, the field distribution of the waveform recorded from the left hemisphere (contralateral to the stimulus) following IES at the peak latency showed a single dipole pattern originating from the upper bank or bottom of the sylvian fissure corresponding to the secondary somatosensory cortex (SII)/insula region, or a two-dipole pattern originating from SII/insula and the primary somatosensory cortex (SI), similar to the results in our previous study following stimulation of the hand (Inui et al., 2002b). In the right hemisphere (ipsilateral to the stimulus), clear magnetic fields were recorded in six subjects and the field distribution showed a single dipole pattern generated by activity from the SII/insula region. Figure 1 shows representative results in the first session. The nine traces in Figure 1A show recorded waveforms in each condition, and the seven traces in Figure 1B show the waveforms obtained by a subtraction of the control TS waveform from the waveform for each of the seven IES + TS conditions. The result of the subtraction clearly showed that cortical responses to IES were markedly attenuated when TS was applied at CTIs of –40, –20, 0 and 50 ms, moderately attenuated at 100 ms and slightly attenuated at 300 and 500 ms. Figures 2 and 3 show the mean time course of the amplitude of the recorded and subtracted waveforms represented as the root mean square (RMS) of all subjects. The mean peak amplitudes of the subtracted waveform of the IES + TS –500, –300, –100, –60, –40, –20, 0, 50, 100, 300 and 500 ms conditions were 100.3 ± 7.1, 100.0 ± 12.2, 99.9 ± 12.8, 76.8 ± 21.4, 34.5 ± 19.6, 20.2 ± 12.7, 23.4 ± 11.3, 35.9 ± 16.5, 45.0 ± 27.2, 68.6 ± 27.0 and 71.0 ± 26.5% of the control response, respectively. The difference among the 11 conditions was significant [$F(1,11) = 27.4$, $P < 0.0001$]. There was a significant linear correlation between the peak amplitude and pain rating (Fig. 4, $r = 0.76$, $P < 0.0001$).
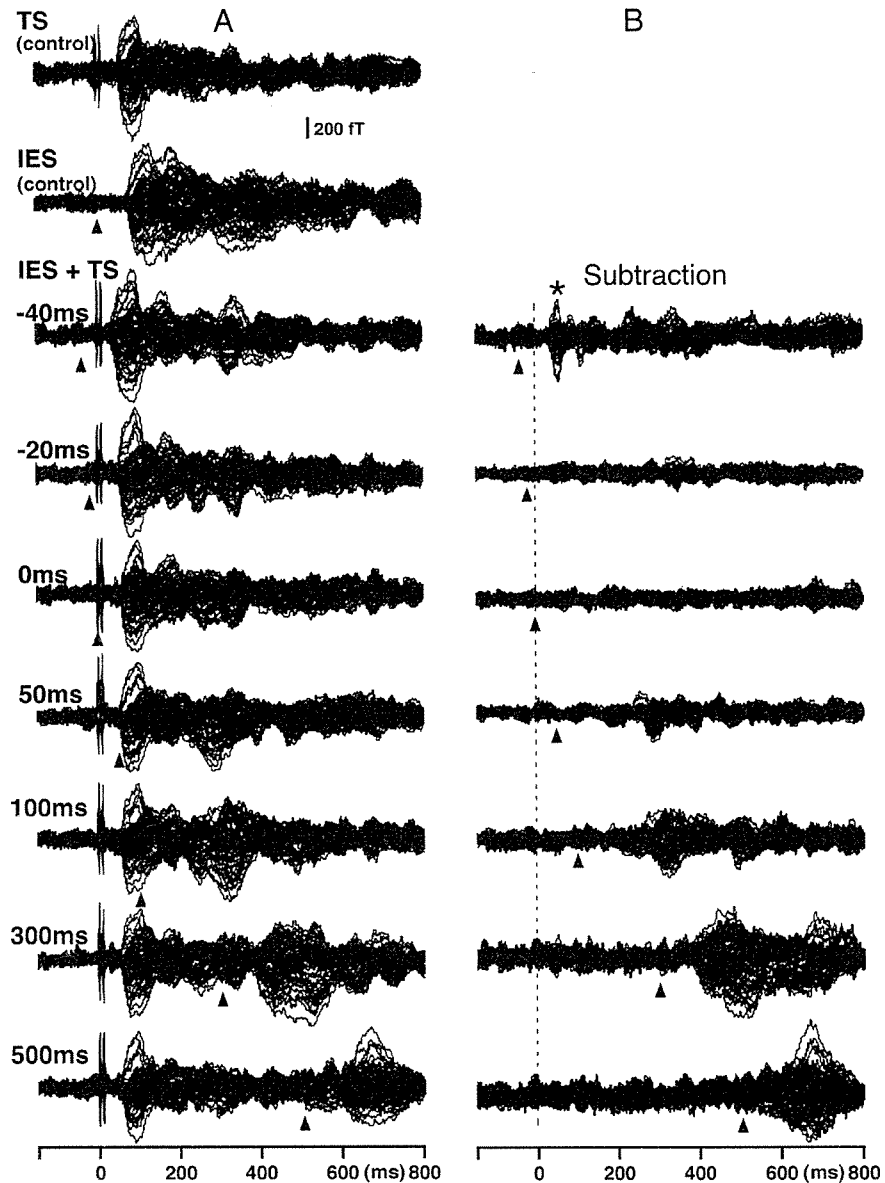
Figure 1. Effects of innocuous somatosensory stimulation on magnetic fields evoked by noxious simulation. (A) Recorded magnetic fields evoked by innocuous stimulation alone (control TS), noxious stimulation alone (control IES) and paired innocuous and noxious stimulations (IES + TS) applied to the back at various CTIs in a single subject (subject 1). Traces are superimposed waveforms recorded from 74 channels. (B) Waveforms obtained by subtraction of the control TS-evoked response from the recorded waveforms in each condition. Filled triangles indicate timing of IES. A sharp component in the subtracted waveform shown by an asterisk indicates that the IES-evoked response occurs earlier than the TS-evoked response in this condition.

Since signals evoked by TS reach the spinal cord ~5 ms earlier than signals evoked by IES due to a difference of peripheral conduction velocity between A-beta and A-delta fibers (see Materials and Methods), signals evoked by IES reach the spinal cord earlier than those due to TS in the IES + TS conditions with negative CTIs >–20 ms. Therefore, data for these IES + TS conditions are important to establishing the level in the central nervous system at which this inhibition occurs. As Figures 1 and 2 show, cortical responses to IES were almost abolished in the IES + TS –20 ms condition, indicating that the inhibition in this condition occurred at a level higher than the spinal cord. In the IES + TS –40 and –60 ms conditions in Figures 1–3, there was a sharp component around 100 ms

after IES shown by an asterisk in the subtracted waveform, which indicated that the IES-induced cortical responses occurred earlier than the TS-induced responses in these conditions, and in addition, large parts of the later IES-evoked responses were almost abolished. Figure 5 shows the difference of waveform in the IES + TS –40 ms condition in detail. The waveform for the IES + TS –40 ms condition was very similar to that of the control TS, suggesting that the cortical response to TS changed little even when signals due to IES reached the cortex slightly early, and that on the other hand, IES-evoked responses were remarkably attenuated by later arriving TS-evoked signals. In Figure 6, waveforms in the IES + TS –40 ms condition of all subjects are shown.
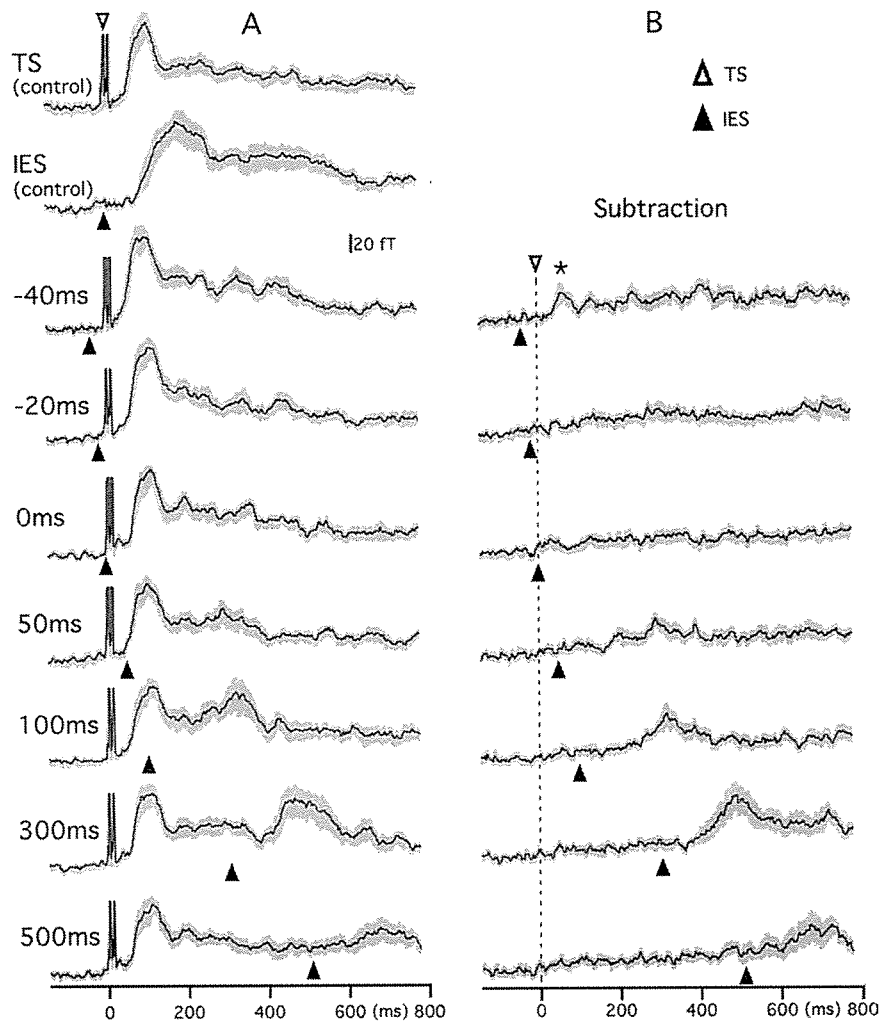
Figure 2. Group-averaged waveforms of the root mean square in the first session with seven IES + TS conditions at a CTI of −40 to 500 ms. Traces are the group-averaged time course of the amplitude of recorded (A) and subtracted (B) waveforms represented as the root mean square across 74 channels. In this and the next figure, shaded areas indicate ±1 SE width.

Next, we calculated how the control TS- and IES-evoked responses explained the waveforms of the IES + TS conditions using a least squares fit. Results from a single subject in Figure 7 showed that the waveform for the IES + TS −40 ms condition was well explained by the TS-evoked response alone except at a latency period ∼50 ms after TS (90 ms after IES) where the IES-evoked response was dominant as shown by an asterisk. The time course of the coefficient *b* for the IES-evoked response was very similar to that of the subtracted waveform at a latency of 40-300 ms, which indicated the reliability of the subtraction method in this condition. Figure 8 depicts group-averaged values of coefficients *a* and *b* as functions of time among all subjects. Among the 11 IES + TS conditions, signals due to IES reach the cortex earlier than those due to TS in the −500 to −40 ms conditions, while signals due to TS reach the cortex earlier in the −20 to 500 ms conditions. Therefore, Figure 8*A,B* compares the effects of later arriving TS signals on the IES-evoked response and effects of later arriving IES signals on the TS-evoked response. On the other hand, Figure 8*C,D* compares the effects of preceding TS signals on the IES-evoked response

and effects of preceding IES signals on the TS-evoked response. It is obvious from Figure 8*B* that later arriving IES signals had almost no effect on the TS-evoked response, while in marked contrast, the IES-evoked responses were strongly inhibited by later arriving TS signals (Fig. 8*A*). In Figure 8*A*, waveforms of coefficient *b* for IES in the −40, −60 and −100 ms conditions started to deviate from that of the −300 or −500 ms condition, which could be considered as a control, at ∼110, 130 and 170 ms after the stimulus, indicating clearly that the IES-evoked responses in these conditions were actively inhibited by later arriving TS signals with a similar timing. In each of the three conditions, the onset latency of the inhibition corresponded approximately to the onset latency of the TS-evoked response plus 20 ms. For example, in the −60 ms condition, the onset latency of the TS-evoked cortical response was expected to be at 110 ms after IES, which was shorter by 20 ms than the latency at which the inhibition started in this condition (130 ms). When the strength of the actual IES-evoked response in each condition was expressed as the area under the curve (AUC, coefficient *b* × ms) during 50-300 ms, the AUCs for the −300,
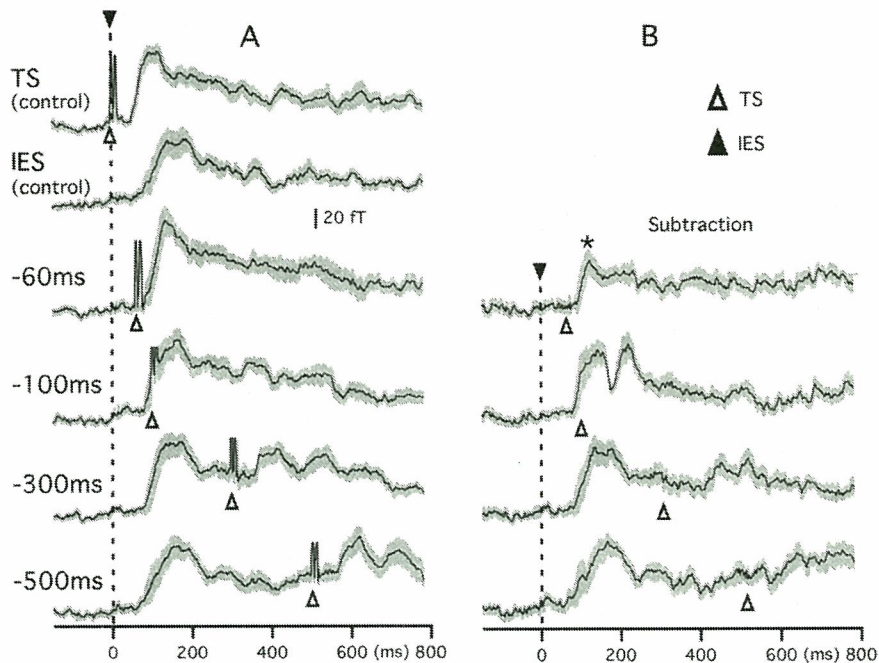
Figure 3. Group-averaged waveforms of the root mean square in the second session with four IES + TS conditions at a CTI of −500 to −60 ms.
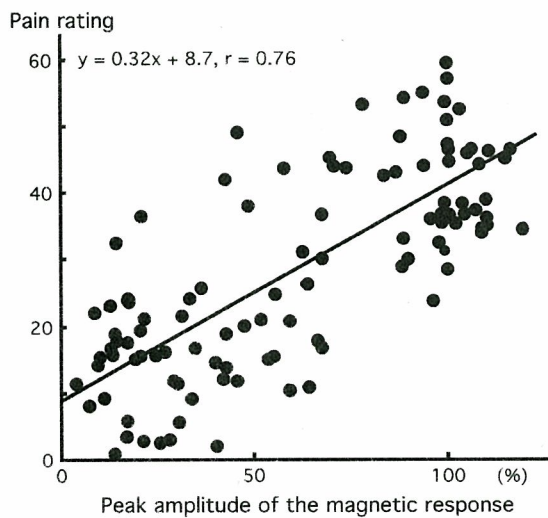

Figure 4. Correlation between the pain rating and peak amplitude of IES-induced cortical response. Data of all stimulus conditions for all subjects are plotted. Amplitudes of magnetic response are represented as a percentage of the control (IES) response. A regression line is indicated.

−100, −60 and −40 ms conditions were 103.9, 78.1, 46.5 and 22.2% of that in the −500 ms condition, respectively (Fig. 9). In the −500 ms condition, the IES-evoked response during 50–300 ms was not affected by TS at all, and therefore could be considered as a control. The AUCs for the TS-evoked response in the −20, 0, 50, 100 and 300 ms condition were 99.0, 97.4, 94.1, 103.0 and 93.1% of that in the 500 ms condition (control).

Figure 8C,D shows that preceding TS signals as well as preceding IES signals inhibited the IES- and TS-evoked responses, respectively. The AUCs for the IES-evoked response in the −20, 0, 50, 100, 300 and 500 ms conditions were 18.3, 15.4,

17.2, 31.6, 40.0 and 30.7% of the control value (−500ms), suggesting that the inhibition continued up to the CTI 500 ms condition. The AUCs for the TS-evoked response in the −500, −300, −100, −60 and −40 ms conditions were 57.5, 69.0, 57.8, 78.2 and 99.1% of the control value. Therefore, the inhibition of the TS-evoked response was not present when the IES- and TS-evoked signals reached the cortex simultaneously (−40 ms condition), appeared when the IES-evoked signals reached the cortex 20 ms earlier than the TS-evoked signals (−60 ms condition) and was strongest when the IES-evoked signals reached the cortex earlier than those due to TS by 60 ms (−100 ms condition). When the degree of the inhibition in these conditions was compared between the TS- and IES-evoked responses, it was significantly stronger for the TS-induced inhibition of the IES-evoked response than the IES-induced inhibition of the TS-evoked response (t-test, $P < 0.0001$). Like the peak amplitude in the RMS analysis, there was a linear correlation between the pain rating and AUC for IES-evoekd responses ($P < 0.0001$, $r = 0.63$). Figure 9 shows the percentage AUC relative to the control for the TS- and IES-evoked response in all conditions.

Discussion

This is the first report to show tactile-induced pain inhibition at the cortical level. A previous paper from our laboratory (Kakigi and Watanabe, 1996) examined effects of tactile stimuli applied to the fingers on vertex potentials evoked by laser beams applied to the dorsum of the same hand. No effects were found when a stroke by a soft wad of tissue paper was used as a tactile stimulus, while laser-evoked potentials were significantly inhibited when continuous vibrotactile stimuli (500 Hz) was used. The results suggest that the timing of the conditioning stimulus is important to its inhibitory effects on pain-evoked brain responses as the present study showed.
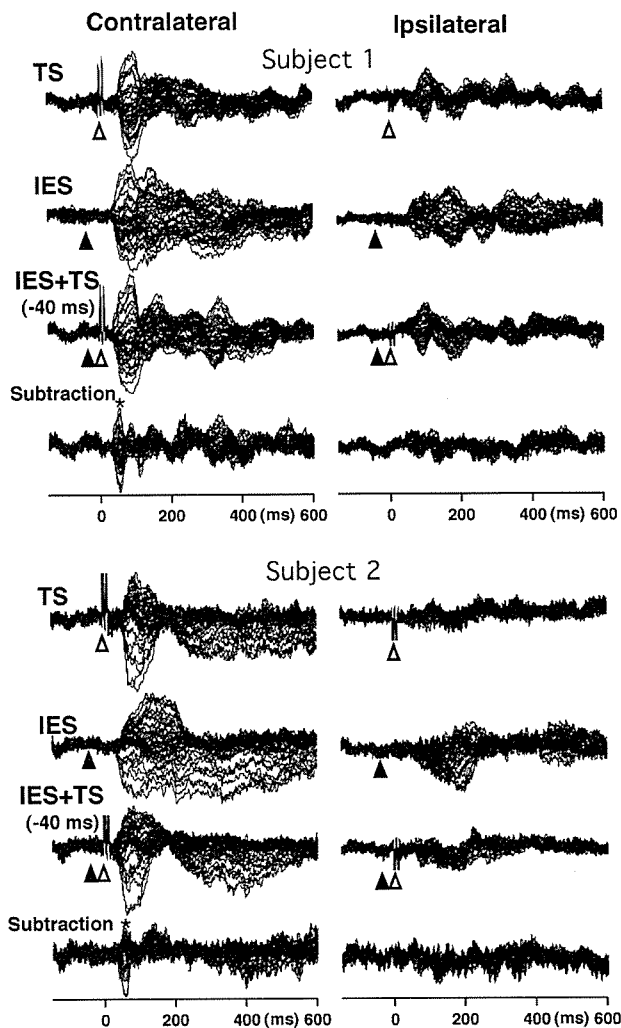
Contralateral   **Ipsilateral**

Figure 5. Inhibition of the IES-evoked response by TS delivered 40 ms later than IES. Waveforms recorded by two probes (contralateral and ipsilateral hemispheres) are separately shown in this figure. Open and filled triangles indicate timing of TS and IES, respectively. Note that waveforms recorded from both hemispheres are very similar between the TS and IES + TS conditions in both subjects except that waveforms in the IES + TS condition have activity due to IES at the very beginning of the evoked component as shown by an asterisk.

It is probable that the failure to find an inhibitory effect of a stroke of the fingers on laser-evoked potentials was due to the non-time-locked conditioning stimuli. An important technical issue of the present study was the use of an intra-epidermal electrical stimulation (IES) method that could selectively activate A-delta fibers with constant activation timing in each trial, and therefore enabled us to study interactions between two different modalities with precise timing. In previous studies, we confirmed that signals evoked by IES are conveyed through peripheral A-delta fibers at a conduction velocity of ~15 m/s (Inui et al., 2002a,b). In this study, the latency difference of evoked cortical activity between TS and IES was ~38 ms, which was almost consistent with the estimated latency difference based on the reported conduction velocities of peripheral A-beta and A-delta signals in the human spinal cord. The sharp pricking sensations without any tactile sensations evoked by IES also support that IES activates A-delta

fibers selectively. Furthermore, the present result itself showed that IES selectively stimulates A-delta fibers. If IES activates A-beta and A-delta fibers simultaneously (i.e. CTI = 0 ms), the responses evoked should be similar in latency to those evoked by TS.

As possible mechanisms underlying pain relief by vibrotactile stimulations, those operating at the periphery (Campbell and Taub, 1973), dorsal horn of the spinal cord (Melzack and Wall, 1965) and other regions of the central nervous system (Melzack, 1971) have been postulated. In the major hypothetical mechanisms at the spinal level, it has been suggested that a 'gate control' mechanism exists in the dorsal horn of the spinal cord, where signals through large diameter fibers are said to inhibit the central transmission of signals through small diameter fibers (Melzack and Wall, 1965). In the present study, noxious stimuli-induced cortical responses were equally inhibited by simultaneous (CTI 0 ms) and delayed (CTI –40 and –20 ms) innocuous stimulations, excluding the possibility of peripheral mechanisms. The findings of a substantial inhibition of the IES-induced response in the IES + TS conditions with a negative CTI of > –20 ms suggest that the inhibition occurs without any contribution at the spinal level, including descending inhibitory actions on spinal neurons, at least in these conditions because signals evoked by IES reach the spinal cord earlier than those evoked by TS. The findings in the IES + TS –100 to –40 ms conditions indicate that the inhibition occurs at the cortical level. Although our results could not clarify the extent to which the spinal mechanisms contributed to the inhibition in the IES + TS 0 to 500 ms conditions, the powerful inhibition in the IES + TS –40 ms and IES + TS –20 ms conditions and the low pain rating for the IES + TS –20 ms condition imply that any inhibitory action at the spinal cord is weak. This notion is consistent with the fact that, in general, repetitive and high intensity stimulations of a peripheral nerve, which activate both A-beta and A-delta fibers, are required to suppress noxious stimuli-evoked responses in the dorsal horn neurons in animal studies (Cervero et al., 1976; Chung et al., 1984; Lee et al., 1985). Whitehorn and Burgess (1973) showed that primary afferent terminals of a particular sensory fiber type are depolarized by activity arising in fibers of the same type. Similar findings were reported by Brown and Hayden (1972). Therefore, inhibition of the nociceptive neurons in the dorsal horn by repetitive stimulation of a peripheral nerve at noxious intensities or by applying intense mechanical stimuli to the skin seems to be largely due to presynaptic inhibition by A-delta or C fiber inputs rather than A-beta fibers. The notion that nociceptive neurons in the dorsal horn cannot be easily suppressed by signals from low-threshold mechanoreceptors is supported by the findings of Manfredi (1970) and Pomeranz (1973), who examined postsynaptic activity of the dorsal horn neurons in the lateral tract in cats and found no inhibitory effects of A-beta fiber inputs. The fact that stimulation of C-fibers generates a primary afferent depolarization but not a primary afferent hyperpolarization in the spinal cord (Zimmermann, 1968) also does not support the gate control theory.

Since the main component of the evoked magnetic fields in the present study originated mainly from SII and SI, and since SI and SII were sequentially activated by IES in our previous study (Inui et al., 2003a,b), the inhibitory action should take place in SI neurons or in both SI and SII neurons. Several lines of evidence show that SI nociceptive neurons play a role in the discriminative aspect of pain (Kenshalo and Willis, 1991;
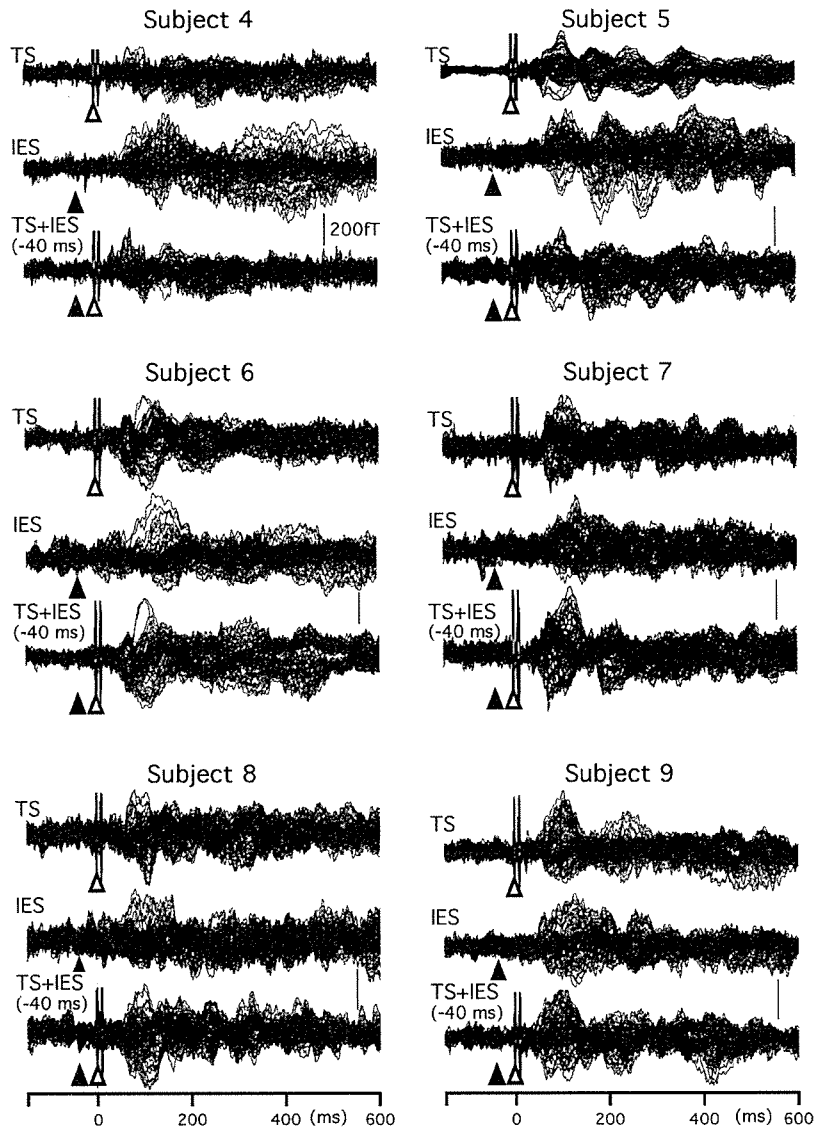
Figure 6. Waveforms in the IES + TS −40 ms condition of six subjects. Note that the waveform in the IES + TS condition is similar to the waveform in the control TS condition. Waveforms of three other subjects in this condition are shown in Figures 1, 5 and 7.

Bushnell *et al.*, 1999). Since the IES-evoked later components, which originated from the insular cortex, medial temporal area around the amygdala or hippocampus and cingulate cortex (Inui *et al.*, 2003a), were attenuated as well as the main early component in this study, there might be direct inhibitory actions on these areas independent of those on SI and SII. The origin of the inhibitory action is unclear from the present results, but TS-driven thalamic and cortical activities are candidates. The present study suggests that activation of the tactile pathway at a certain level higher than that in the spinal cord can inhibit cortical responses to noxious stimuli. In the major tactile pathway, the dorsal column is known to alleviate chronic pain when electrically stimulated (Shealy *et al.*, 1970). In addition, behavioral responses to noxious stimuli in rats (Saadé *et al.*, 1986) as well as experimentally evoked pain in humans (Marchand *et al.*, 1991) are reduced by stimulation of the dorsal column. Although the mechanisms responsible for

pain inhibition on stimulation of the dorsal column are still unclear, the nociceptive thalamus–SI pathway might be modulated. Larson *et al.* (1974) showed that evoked potentials recorded in human somatosensory cortex, and those recorded in monkey ventroposterior lateral nucleus (VPL) of the thalamus and sensorimotor cortex are attenuated by stimulation of the dorsal column. Bantli *et al.* (1975) examined the effects stimulating the dorsal column on the cortical responses to stimulation of the ventral quadrant of the spinal cord in monkeys and found that evoked activities in both SI and SII were inhibited, similar to the present results.

In the main tactile pathway, the VPL and the ventroposterior medial nucleus (VPM) of the thalamus are shown to reduce experimentally induced pain in humans when electrically stimulated (Marchand *et al.*, 2003). In addition, electrical stimulation of VPL/VPM is effective in relieving chronic pain (Hosobuchi *et al.*, 1973; Mazars *et al.*, 1973) and allodynia
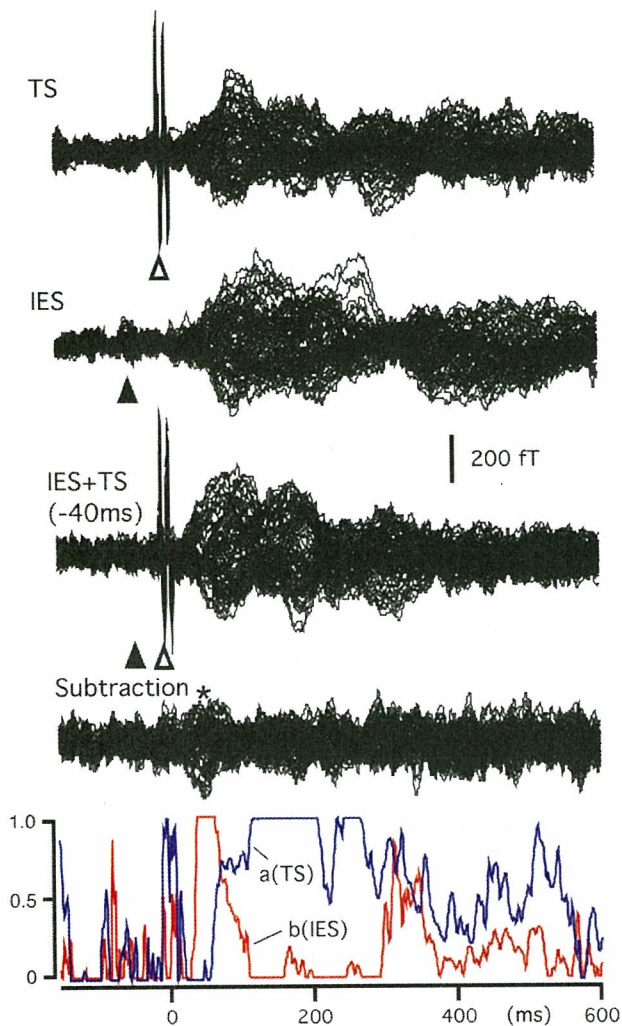
Figure 7. Contribution of the control TS- and IES-evoked responses to the responses evoked by paired stimuli. By use of a least squares fit, we calculated how the control TS and IES waveforms explained the waveforms in IES + TS conditions. The bottom traces show the time course of coefficients for TS (a) and IES (b). The result of this case (subject 3) shows that magnetic fields evoked by paired stimuli can be explained by only the control TS-evoked response except at a latency period of ~30–60 ms after TS, where the control IES-evoked response alone can explain the response shown by an asterisk.

in rats (Kupers and Gybels, 1993). Like stimulation of the peripheral nerve and dorsal column, the stimulation of VPL/VPM usually elicits paresthetic sensations without sensations of pain. In addition, the electrode must be placed in the somatotopic part of the VPL/VPM nuclei that represents the painful site to obtain pain relief (Gybels, 2001), which mimics rubbing a bruised area to reduce pain. These thalamic nuclei send dense projections to SI. Therefore, this thalamo-cortical pathway may mediate analgesia produced by thalamic stimulation. The fact that successful stimulation in patients with chronic pain produces localized paresthetic sensations in the painful area and increases cerebral blood flow in SI and the thalamic region stimulated (Katayama et al., 1986; Duncan et al., 1998) appears to support the involvement of the VPL/VPM-SI pathway in pain relief by thalamic stimulation. The inhibition of nociceptive SI neurons by sensory thalamus

stimulation may explain why electrical stimulation of this area rarely produces painful sensations though VPL/VPM contains considerable numbers of nociceptive neurons (Kenshalo et al., 1980; Chung et al., 1986; Bushnell et al., 1993; Apkarian and Shi, 1994). Davis et al. (1996) examined effects of microstimulation in the ventrocaudal nucleus of the thalamus of patients with chronic pain and found that the stimulation frequently evoked sensations of pain in patients with post-stroke pain but only paresthetic sensations in non-stroke patients. The increased incidence of thalamic-evoked pain in such patients may be due to the relative dominance of the nociceptive thalamus-SI pathway following loss of low-threshold mechanoreceptor thalamic neurons or reduced tonic inhibition of thalamic or cortical nociceptive neurons. This notion is similar to Mazars's original hypothesis of pain relief by thalamic stimulation that when pain is due to a lack of proprioceptive information reaching the thalamus from the damaged region, it might be controlled by thalamic stimulation in place of physiological stimuli running through the dorsal column.

Another possible explanation of tactile-induced pain inhibition is that tactile inputs inhibit nociceptive brain areas other than the VPL–SI pathway via thalamo-thalamic, thalmo-cortical or cortico-cortical inhibitory projections. For example, Craig et al. (1994) demonstrated a very high concentration of pain- and thermo-specific neurons in the posterior part of the ventral medial thalamic nucleus (VMpo) in monkeys, which has dense lamina I spinothalamic tract terminations. In lamina I of the dorsal horn, there is a population of neurons specifically responding to noxious stimuli in cats (Christensen and Perl, 1970) and monkeys (Kumazawa et al., 1975) similar to VMpo neurons. In addition, stimulation around VMpo elicits localized sharp painful sensations and nociceptive-specific neurons are recorded in this region in humans (Craig, 2003). VMpo projects to the dorsal part of the insula and other cortical areas such as area 3a of SI (Craig, 2003). Therefore, VMpo and its projection sites may be the target in tactile-induced inhibition of pain. We considered that a thalamo-cortical pathway via VMpo is one candidate for sites receiving inhibitory effects, although some recent studies questioned the existence of this nucleus (Willis et al., 2002).

Previous studies suggested one primary site of pain processing in the dorsal posterior insula (Craig, 2003; Vogel et al., 2003) where VMpo projects. In fact, activity from the dorsal part of the insula contributes to creating the major magnetic component evoked by IES (Inui et al., 2003a), which was almost completely suppressed by TS in the present study. As for activity in area 3a, Tommerdahl et al. (1996) demonstrated clusters of nociceptive neurons that show an augmenting response to repeated brief heat stimuli in monkeys. In addition, they showed that activation in area 3a by noxious heat stimuli was accompanied by a reduction of activity in areas 3b and 1 produced by innocuous mechanical simulation, which was likely mediated by long-distance horizontal connections that link area 3a and areas 3b/1. Given the inhibitory cortico-cortical projections from area 3a to areas 3b/1 in the pain-touch interaction, it seems possible that IES-evoked area 3a activity was inhibited by similar cortico-cortical projections from areas 3b/1 in the present study. Our data that the onset latency of the inhibition of the IES-evoked response by TS was ~20 ms later than the arrival of TS signals to the cortex (IES +TS conditions from –100 to –40 ms) are consistent with such a cortico-cortical inhibition. However, activation of neurons in the bottom of the sulcus creates
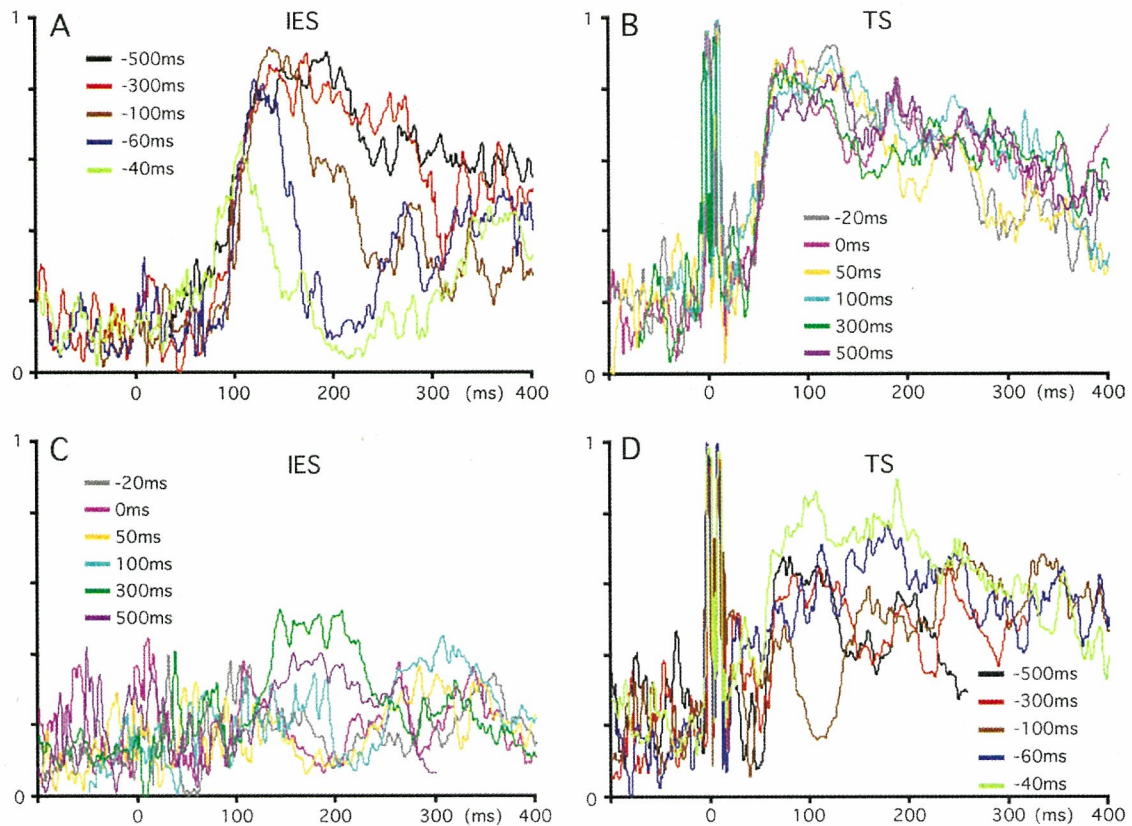
Figure 8. Group-averaged time course of the coefficients for TS and IES. (*A*) Effects of later arriving TS signals on the IES-evoked response. (*B*) Effects of later arriving IES signals on the TS-evoked response. (*C*) Effects of preceding TS signals on the IES-evoked response. (*D*) Effects of preceding IES signals on the TS-evoked response.

a dipole with a radial orientation that is difficult detect by MEG, therefore our recorded magnetic fields might not reflect activity from area 3a.

The role of SII in pain perception is unclear, largely due to the lack of unit study findings on nociceptive neurons in this area. In marked contrast with human neuroimaging studies in which activations in SII are constantly found after noxious stimulation, nociceptive neurons are rarely encountered in SII in animal studies (for review, see Schnitzler and Ploner, 2000). For example, the proportion of nociceptive neurons was 4% (5 of 123 neurons) in a study by Dong *et al.* (1989). The present finding of powerful inhibition by tactile inputs of responses to noxious stimuli in SII suggests that the paucity of nociceptive neurons in SII in animal studies might be a result of the use of a non-selective intense mechanical stimulation that activates low-threshold mechanoreceptors as well as nociceptors, since the present results showed that noxious stimuli-evoked SII activity was markedly inhibited when an innocuous stimulus was applied simultaneously (CTI 0 ms). If a selective noxious stimulation is used as a searching stimulus, a larger number of nociceptive neurons might be found in SII.

Although the pain rating was correlated with both the peak amplitude of the IES-evoked response (subtracted) and the integral strength of the coefficient for the IES-evoked response during the 50–300 ms latency, data in some conditions did not show a simple linear correlation between them. The rating for the IES + TS –40 ms condition (12.7) was not so different from that for the –20 ms (11.1) and 0 ms (13.7) conditions, while
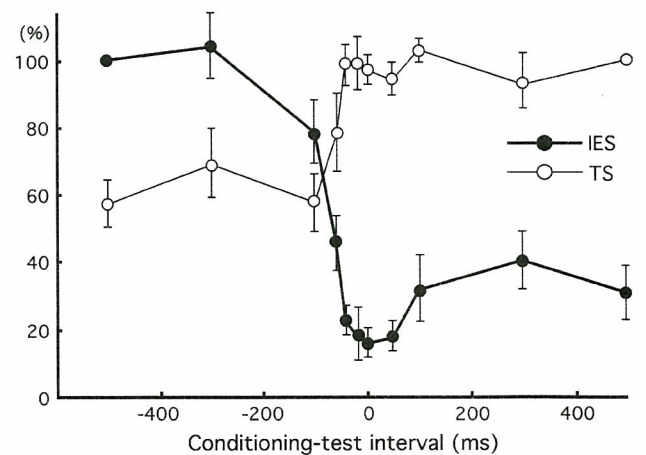

Figure 9. Amplitudes of the IES- and TS-evoked response represented as an integral of the respective coefficient value. Each value is the percentage of the area under the curve (AUC) during a latency period of 50–300 ms relative to that in the control condition (500 ms condition for TS and −500 ms condition for IES). Vertical bars indicate ±1 SE.

the peak amplitude of the –40 ms condition (34.5% of the control) was apparently greater than that of the –20 ms (20.2%) and 0 ms (23.4%) conditions, due to the presence of an early sharp component that escaped the inhibition in the –40 ms condition. This result implies that the early sharp component in the –40 ms condition did not help to produce painful sensations.

We considered that the early activity in the -40 ms condition with a very short duration (shown by an asterisk) was not sufficient to evoke painful sensations, that is, below the level critical to drive the subsequent processing related with pain recognition or pain rating in amplitude or in duration. In contrast, the rating in the -60 ms condition (37.4) was much larger than that in the -40, -20 and 0 ms conditions, suggesting that the strength or duration of the early activity in this condition might exceed the critical level.

Although the present study found an inhibitory effect of noxious stimulus on the tactile-evoked cortical response, its manner was strikingly different from that observed in the IES-induced inhibition of the TS-evoked response in that the IES-evoked cortical response was strongly inhibited by later arriving TS signals whereas inhibitory effects of IES signals on the TS-evoked response were observed only when the IES signals preceded the TS signals. Therefore, there is a specific one-way touch-pain inhibitory action although the inhibitory effects of a preceding activation of one modality on the other may be reciprocal. The stronger inhibition of the IES-evoked response (Fig. 8C) than TS-evoked response (Fig. 8D) might be because the inhibition of the IES-evoked response was a summation of the specific touch-pain inhibitory action and a weaker reciprocal inhibitory mechanism. The inhibitory effect of pain on tactile processing is consistent with previous findings that tonic pain elevated vibrotactile perception thresholds (Apkarian et al., 1994; Bolanowski et al., 2000) and decreased proprioception (Rossi et al., 1998), and that innocuous tactile stimulation-induced activations in SI (3b and 1) were decreased during heat pain in monkeys (Tommerdahl et al., 1996), although the mechanism of the inhibition might be different from that observed in this study, since the present study used a phasic pain stimulus instead of tonic pain. A few neurophysiological studies have assessed effects of pain on tactile processing using a phasic painful conditioning stimulus. In an MEG study, Tran et al. (2003) compared the effects of conditioning innocuous and noxious electrical stimulations to the finger on cortical responses to median nerve stimulation and found that noxious stimulation elicited greater effects in reducing the early SI activity evoked by median nerve stimulation at CTIs of 100–400 ms, indicating that activation of A-delta fibers significantly inhibited the cortical tactile response. On the other hand, Dowman (1999) and Ploner et al. (2004) used brief painful laser stimuli to examine touch-pain interaction and found an augmentation of tactile processing. However, both studies examined only one CTI (194 and 500 ms, respectively) and therefore could not assess the effects of conditioning noxious stimuli at various timings.

Although activities of nociceptive neurons in the dorsal horn have been shown to be modulated under various conditions, including segmental sensory stimulation (Handwerker and Zimmermann, 1975), noxious stimulation applied to various parts of the body (Le Bars et al., 1979; Gerhart et al., 1981), thalamic stimulation (Gerhart et al., 1983) and dorsal column stimulation (Handwerker and Zimmermann, 1975; Foreman et al., 1976), our results indicate that powerful modulation also occurs in the brain. There are surprisingly few studies dealing with such inhibitory mechanisms in the brain. This apparently shows that past studies have stressed the spinal mechanism of pain modulation. We consider that mechanisms in the brain as well as the spinal cord should be taken into consideration in both experimental and clinical studies.

There should be various types of modulation at various levels that interact with each other.

Notes

References

Apkarian AV, Shi T (1994) Squirrel monkey lateral thalamus. I. Somatic nociresponsive neurons and their relation to spinothalamic terminals. J Neurosci 14:6779-6795.

Apkarian AV, Stea RA, Bolanowski SJ (1994) Heat-induced pain diminishes vibrotactile perception: a touch gate. Somatosens Motor Res 11:259-267.

Bantli H, Bloedel JR, Thienprasit P (1975) Supraspinal interactions resulting from experimental dorsal column stimulation. J Neurosurg 42:296-300.

Bolanowski SJ, Maxfield LM, Gescheider GA, Apkarian AV (2000) The effects of stimulus location on the gating of touch by heat- and cold-induced pain. Somatosens Motor Res 17:195-204.

Brown AG, Hayden RE (1972) Presynaptic depolarization produced by and in identified cutaneous afferent fibres in the rabbit. Brain Res 38:187-192.

Bushnell MC, Duncan GH, Tremblay N (1993) Thalamic VPM nucleus in the behaving monkey. I. Multimodal and discriminative properties of thermosensitive neurons. J Neurophysiol 69:739-752.

Bushnell MC, Duncan GH, Hofbauer RK, Ha B, Chen J-I, Carrier B (1999) Pain perception: is there a role for primary somatosensory cortex? Proc Natl Acad Sci USA 96:7705-7709.

Campbell JN, Taub A (1973) Local analgesia from percutaneous electrical stimulation. A peripheral mechanism. Arch Neurol 28:347-350.

Cervero F, Iggo A, Ogawa H (1976) Nociceptor-driven dorsal horn neurons in the lumbar spinal cord of the cat. Pain 2:5-24.

Christensen BN, Perl ER (1970) Spinal neurons specifically excited by noxious or thermal stimuli: marginal zone of the dorsal horn. J Neurophysiol 33:293-307.

Chung JM, Lee KH, Hori Y, Endo K, Willis WD (1984) Factors influencing peripheral nerve stimulation produced inhibition of primate spinothalamic tract cells. Pain 19:277-293.

Chung JM, Lee KH, Surmeirer DJ, Sorkin LS, Kim L, Willis WD (1986) Response characteristics of neurons in the ventral posterior lateral nucleus of the monkey thalamus. J Neurophysiol 56:370-390.

Craig AD (2003) Pain mechanisms:labeled lines versus convergence in central processing. Annu Rev Neurosci 26:1-30.

Craig AD, Bushnell MC, Zhang E-T, Blomqvist A (1994) A thalamic nucleus specific for pain and temperature sensation. Nature 372:770-773.

Davis KD, Kiss ZHT, Tasker RR, Dostrovsky JO (1996) Thalamic stimulation-evoked sensations in chronic pain patients and in non-pain (movement disorder) patients. J Neurophysiol 75:1026-1037.

Dong WK, Salonen LD, Kawakami Y, Shiwaku T, Kaukoranta EM, Martin RF (1989) Nociceptive responses of trigeminal neurons in SII-7b cortex of awake monkeys. Brain Res 484:314-324.

Dowman R (1999) Laser pain fails to inhibit innocuous-related activity in the central somatosensory pathways. Psychophysiology 36: 371-378.

Duncan GH, Kupers RC, Marchand S, Villemure J-G, Gybers JM, Bushnell MC (1998) Stimulation of human thalamus for pain relief:possible modulatory circuits revealed by positron emission tomography. J Neurophysiol 80:3326-3330.

Foreman RD, Beall JE, Applebaum AE, Coulter JD, Willis WD (1976) Effects of dorsal column stimulation on primate spinothalamic tract neurons. J Neurophysiol 39:534-546.

Gerhart KD, Yezierski RP, Giesler GJ Jr, Willis WD (1981) Inhibitory receptive fields of primate spinothalamic tract cells. J Neurophysiol 46:1309-1325.

Gerhart KD, Yezierski RP, Fang ZR, Willis WD (1983) Inhibition of primate spinothalamic tract neurons by stimulation in ventral posterior lateral (VPLc) thalamic nucleus: possible mechanisms. J Neurophysiol 49:406–423.

Gybels J (2001) Thalamic stimulation in neuropathic pain: 27 years later. Acta Neurol Belg 101:65–71.

Handwerker HO, Zimmermann M (1975) Segmental and supraspinal actions on dorsal horn neurons responding to noxious and non-noxious skin stimuli. Pain 1:147–165.

Hosobuchi Y, Adams JE, Rutkin B (1973) Chronic thalamic stimulation for the control of facial anesthesia dolorosa. Arch Neurol 29:158–161.

Inui K, Tran DT, Hoshiyama M, Kakigi R (2002a) Preferential stimulation of Aδ fibers by intra-epidermal needle electrode in humans. Pain 96:247–252.

Inui K, Tran DT, Qiu Y, Wang X, Hoshiyama M, Kakigi R (2002b) Pain-related magnetic fields evoked by intra-epidermal electrical stimulation in humans. Clin Neurophysiol 113:298–304.

Inui K, Tran DT, Qiu Y, Wang X, Hoshiyama M, Kakigi R (2003a) A comparative magnetoencephalographic study of cortical activations evoked by noxious and innocuous somatosensory stimulations. Neuroscience 120:235–248.

Inui K, Wang X, Qiu Y, Nguyen BT, Ojima S, Tamura Y, Nakata H, Wasaka T, Tran TD, Kakigi R (2003b) Pain processing within the primary somatosensory cortex in humans. Eur J Neurosci 18:2859–2866.

Kakigi R, Shibasaki H (1991) Estimation of conduction velocity of the spino-thalamic tract in man. Electroencephalogr Clin Neurophysiol 80:39–45.

Kakigi R, Watanabe S (1996) Pain relief by various kinds of interference stimulation applied to the peripheral skin in humans: pain-related brain potentials following CO_2 laser stimulation. J Peripher Nerv Syst 1:189–198.

Kakigi R, Hoshiyama M, Shimojo M, Naka D, Yamasaki H, Watanabe S, Xiang J, Maeda K, Lam K, Itomi K, Nakamura A (2000) The somatosensory evoked magnetic fields. Prog Neurobiol 61:495–523.

Katayama Y, Tsubokawa T, Hirayama T, Kido G, Tsukiyama T, Iio M (1986) Response of regional cerebral blood flow and oxygen metabolism to thalamic stimulation in humans as revealed by positron emission tomography. J Cereb Blood Flow Metab 6:637–641.

Kenshalo DR Jr, Willis WD Jr (1991) The role of the cerebral cortex in pain sensation. In: Cerebral cortex. Vol. 9. Normal and altered states of function (Peters A, Jones EG, eds), pp. 153–212. New York: Plenum Press.

Kenshalo DR Jr, Giesler GJ Jr, Leonard RB, Willis WD (1980) Responses of neurons in primate ventral posterior lateral nucleus to noxious stimuli. J Neurophysiol 43:1594–1614.

Kumazawa T, Perl ER, Burgess PR, Whitehorn D (1975) Ascending projections from marginal zone (lamina I) neurons of the spinal dorsal horn. J Comp Neurol 162:1–12.

Kupers RC, Gybels JM (1993) Electrical stimulation of the ventroposterolateral thalamic nucleus (VPL) reduces mechanical allodynia in a rat model of neuropathic pain. Neurosci Lett 150:95–98.

Larson SJ, Sances A Jr, Riegel DH, Meyer GA, Dallmann DE, Swiontek T (1974) Neurophysiological effects of dorsal column stimulation in man and monkey. J Neurosurg 41:217–223.

Le Bars D, Dickenson AH, Besson JM (1979) Diffuse noxious inhibitory controls (DNIC) I. Effects on dorsal horn convergent neurons in the rat. Pain 6:283–304.

Lee KH, Chung JM, Willis WD (1985) Inhibition of primate spinothalamic tract cells by TENS. J Neurosurg 62:276–287.

Manfredi M (1970) Modulation of sensory projections in anterolateral column of cat spinal cord by peripheral afferents of different size. Arch Ital Biol 108:72–105.

Marchand S, Bushnell MC, Molina-Negro P, Martinez SN, Duncan GH (1991) The effects of dorsal column stimulation on measures of clinical and experimental pain in man. Pain 45:249–257.

Marchand S, Kupers RC, Bushnell MC, Duncan GH (2003) Analgesic and placebo effects of thalamic stimulation. Pain 105:481–488.

Mazars G, Mérienne L, Ciolocca C (1973) Stimulations thalamiques intermittentes antalgiques. Note préliminaire. Rev Neurol Paris 128:273–279.

Melzack R (1971) Phantom limb pain: implications for treatment of pathologic pain. Anesthesiology 35:409–419.

Melzack R, Wall PD (1965) Pain mechanisms: a new theory. Science 150:971–979.

Meyer GA, Fields HL (1972) Causalgia treated by selective large fibre stimulation of peripheral nerve. Brain 95:163–168.

Ploner M, Pollok B, Schnitzler A (2004) Pain facilitates tactile processing in human somatosensory cortices. J Neurophysiol 92:1825–1829.

Pomeranz B (1973) Specific nociceptive fibers projecting from spinal cord neurons to the brain:a possible pathway for pain. Brain Res 50:447–451.

Rossi A, Decchi B, Groccia R, Della Volla R, Spidalieri r (1998) Interactions between nociceptive and non-nociceptive afferent projections to cerebral cortex in humans. Neurosci Lett 248:155–158.

Saadé NE, Tabet MS, Soueidan SA, Bitar M, Atweh SF, Jabbur SJ (1986) Supraspinal modulation of nociception in awake rats by stimulation of the dorsal column nuclei. Brain Res 369:307–310.

Schnitzler A, Ploner M (2000) Neurophysiology and functional neuroanatomy of pain perception. J Clin Neurophysiol 17:592–603.

Shealy CN, Mortimer JT, Hagfors NR (1970) Dorsal column electroanalgesia. J Neurosurg 32:560–564.

Tommerdahl M, Delemos KA, Vierck CJ Jr, Favorov OV, Whitsel BL (1996) Anterior parietal cortical response to tactile and skin-heating stimuli applied to the same skin site. J Neurophysiol 75:2662–2670.

Tran TD, Hoshiyama M, Inui K, Kakigi R (2003) Electrical-induced pain diminishes somatosensory evoked magnetic cortical fields. Clin Neurophysiol 114:1704–1714.

Vogel H, Port JD, Lenz F, Solaiyappan M, Kauss G, Treede RD (2003) Dipole source analysis of laser-evoked subdural potentials recorded from parasylvian cortex in humans. J Neurophysiol 89:3051–3060.

Wall PD, Cronly-Dillon JR (1960) Pain, itch, and vibration. Arch Neurol 2:365–375.

Wall PD, Sweet WH (1967) Temporary abolition of pain in man. Science 155:108–109.

Whitehorn D, Burgess PR (1973) Changes in polarization of central branches of myelinated mechanoreceptor and nociceptor fibers during noxious and innocuous stimulation of the skin. J Neurophysiol 36:226–237.

Willis WD Jr, Zhang X, Honda CN, Giesler GJ Jr (2002) A critical review of the role of the proposed VMpo nucleus in pain. J Pain 3:79–94.

Woolf CJ, Barrett GD, Mitchell D, Myers RA (1977) Naloxone-reversible peripheral electroanalgesia in intact and spinal rats. Eur J Pharmacol 45:311–314.

Zimmermann M (1968) Dorsal root potentials after C-fiber stimulation. Science 160:896–898.

Brain Processing of the Signals Ascending Through Unmyelinated C Fibers in Humans: An Event-Related Functional Magnetic Resonance Imaging Study

Yunhai Qiu[1,3], Yasuki Noguchi[1,3], Manabu Honda[2,3,4], Hiroki Nakata[1,3], Yohei Tamura[1], Satoshi Tanaka[2,3], Norihiro Sadato[2,3,4], Xiaohong Wang[1], Koji Inui[1,3] and Ryusuke Kakigi[1,3,5]

[1]Department of Integrative Physiology and [2]Division of Cerebral Integration, National Institute for Physiological Sciences, Myodaiji, Okazaki 444-8585, Japan, [3]Department of Physiological Sciences, School of Life Sciences, The Graduate University for Advanced Studies, Hayama, Kanagawa 240-0193, Japan and [4]SORST and [5]RISTEX, Japan Science and Technology Corp Agency (JST), Kawaguchi 332-0012, Japan

Event-related functional magnetic resonance imaging was used to investigate brain processing of the signals ascending from peripheral C and Aδ fibers evoked by phasic laser stimuli on the right hand in humans. The stimulation of both C and Aδ nociceptors activated the bilateral thalamus, bilateral secondary somatosensory cortex, right (ipsilateral) middle insula, and bilateral Brodmann's area (BA) 24/32, with the majority of activity found in the posterior portion of the anterior cingulate cortex (ACC). However, magnitude of activity in the right (ipsilateral) BA32/8/6, including dorsal parts in the anterior portion of the ACC (aACC) and pre-supplementary motor area (pre-SMA), and the bilateral anterior insula was significantly stronger following the stimulation of C nociceptors than Aδ nociceptors. It was concluded that the activation of C nociceptors, related to second pain, evokes different brain processing from that of Aδ nociceptors, related to first pain, probably due to the differences in the emotional and motivational aspects of either pain, which are mainly related to the aACC, pre-SMA, and anterior insula.

Keywords: ACC (anterior cingulate cortex), Aδ fiber, C fiber, fMRI, pain

Introduction

Generally, acute pain is classified as first and second pain associated with rapidly conducting Aδ fibers and slowly conducting unmyelinated C fibers, respectively. First pain aims at achieving relative safety from the source of injury, whereas second pain, with its strong affective component, attracts longer lasting attention and initiates behavioral responses in order to limit further injury and optimize recovery (Wall 1979; Ploner and others 2002). Accordingly, the distinct brain representations for first and second pain should reflect distinct biological functions of both sensations.

Because a phasic painful laser pulse can produce brain responses related to first pain (Mor and Carmon 1975), pain perception in humans has been intensively investigated in neuroimaging studies using positron emission tomography (PET) and functional magnetic resonance imaging (fMRI). Using conventional laser stimuli, these studies showed activations in multiple regions such as the primary somatosensory cortex (SI), secondary somatosensory cortex (SII), insula cortex, and cingulate cortex (Svensson and others 1997; Xu and others 1997; Mauguiere and others 1999; Sawamoto and others 2000; Bingel and others 2002; Bornhovd and others 2002; Buchel and others 2002; Bingel, Glascher, and others 2004; Bingel, Lorenz, and others 2004). However, the differential brain responses to signals ascending from peripheral Aδ and C fibers are unclear and remain to be investigated because these neuroimaging studies only investigated brain processing on the activation of Aδ nociceptors. Although painful laser pulses activate concomitantly Aδ and C nociceptors, it was very difficult or impossible to

activate C nociceptors independently using laser stimulation (Bromm and Treede 1984).

To examine brain processing related to the activation of C nociceptors, capsaicin injection has been employed in a few neuroimaging studies using PET and fMRI. However, capsaicin is associated with the stimulation of not only C nociceptors but also Aδ nociceptors (Holzer 1991; Szallasi 1994), and the responses it evokes reflect a mixture of bottom–up and top–down processes and complex pain-coping strategies, as well as perceptual and physiological phenomena like temporal summation (Price and others 1977) and wind up (Mendell and Wall 1965) because capsaicin induces long-lasting tonic pain. Therefore, using phasic (short lasting) stimulation to selectively activate C nociceptors is more suitable to the study of brain processing based on identification of the onset period for laser stimuli and fMRI scans than tonic capsaicin-induced stimulation.

Recently, a Belgian group (Bragard and others 1996; Opsommer and others 1999) developed a new method for selectively stimulating C nociceptors using a laser pulse applied to a tiny area of skin and succeeded in recording laser-evoked potentials (LEPs) related to the activation of C nociceptors (Plaghki and Mouraux 2003). The physiological background of this method is that the C nociceptors in the skin have a higher density than the Aδ nociceptors (Ochoa and Torebjork 1989; Schmidt and others 1994; Treede and others 1994). We adopted this new approach by arranging the stimulus method. We used an aluminum plate with many holes whereas the Belgian group used a plate with 1 hole attached at the top of the laser stimulation probe. We concluded that this method selectively activates C nociceptors based on studies using microneurography (Qiu and others 2003), electroencephalography (EEG) (Qiu and others 2001, 2002; Tran and others 2001; Tran and others 2003), and magnetoencephalography (Tran and others 2002; Qiu and others 2004).

In this study, we used fMRI to identify brain activity evoked by the stimulation of C nociceptors using an aluminum plate with numerous holes in healthy human subjects. We also used fMRI following the activation of Aδ nociceptors with a conventional method (without using the aluminum spatial filter) to compare the results between the 2 methods. This procedure should demonstrate the distinct brain responses reflecting different biological functions of both first and second pain.

Methods

Subjects

Thirteen healthy male volunteers (1 left handed) participated in this study. They ranged in age from 25 to 39 (mean ± standard deviation: 30.9 ± 4.3). This study was approved by the Ethics Committee at our Institute, and all participants gave their informed consent. None of the

subjects suffered from diseases that might affect normal somatosensory and pain perception. During scanning, 1 investigator stayed with the subject in the scanner room and applied the laser stimuli to the dorsum of the right hand.

Stimulation of C and Aδ Nociceptors

A Tm:YAG laser stimulator (Carl Baasel Lasertech, Starnberg, Germany) was used to apply brief radiant pulses to the skin of the subjects with a wavelength of 1960 nm, a pulse duration of 1 ms, and a spot diameter of 3 mm. For stimulating C nociceptors, we used a thin aluminum plate attached to the top of the stimulus probe (distal end of laser optical fiber) as a spatial filter. This filter was 0.1 mm in depth, and in an area of 10×10 mm^2 on this plate, parallel lines were drawn every 1 mm, giving 11×11 intersections. A total of 121 (11×11) thin holes were drilled at these intersections, each with a diameter of 0.4 mm, corresponding to an area of 0.125 mm^2 for each hole. The laser pulse penetrated 7-11 holes on average. This aluminum spatial filter was placed as close as possible (less than 2 mm) above the skin to reduce the effect of diffraction. The principle of this method was based on that of previous studies (see Kakigi and others 2003; Plaghki and Mouraux 2003). For stimulating Aδ nociceptors, we used conventional laser stimuli without using the aluminum spatial filter. Because stimulus duration was very short, 1 ms, subjects felt a sharp (Aδ fibers stimulation) and burning or dull (C fibers stimulation) pain for a short period.

Before fMRI scanning, we determined the stimulus intensity for each subject by recording LEPs by averaging EEG. Bragard and others (1996) used 2 different laser strengths for activating C nociceptors, one weaker than and one the same as that for Aδ nociceptors, and recorded similar LEP findings between them. However, to minimize the effect of a difference of laser strength, we used the same laser strength for activating C and Aδ nociceptors, though the energy absorbed in the skin might not be exactly the same because of the spatial filter used for activating C nociceptors. The laser strength was determined as the weakest that could evoke clear LEPs following the stimulation of both C (using a thin aluminum plate) and Aδ (conventional method) nociceptors in each subject to minimize skin damage and discomfort (Qiu and others 2004). The mean intensity was 159.6 mJ, ranging from 145.0 to 180.0 mJ. The mean peak latency of the main positive component of LEPs following the stimulation of Aδ and C nociceptors was 351.1 and 932.2 ms, respectively. Using this procedure, we had confirmed that the present stimulus method was appropriate before recording fMRI.

Experimental Paradigm and Imaging Acquisition

The experiment was performed on 2 different days, with the second experiment performed 7 days after the first. In the first experiment, the 13 subjects were randomly separated into 2 groups, one assigned to the examination that stimulated C nociceptors, the other assigned to the examination that stimulated Aδ nociceptors. During the second experiment, these groups were switched. The event-related (single-event) design was used in this study. During the fMRI scans, the laser for either Aδ or C stimulation was applied to the right hand of subjects. The interstimulus interval between adjacent stimuli was either 14, 16, or 18 s, and these intervals were controlled with stimulus presentation software (Presentation 0.50, Neurobehavioral Systems, Albany, California). The fMRI scans were acquired using blood oxygenation level-dependent contrast T2*-weighted gradient echo. A total of 248 fMRI scans per session were acquired using echo-planar imaging sequences (time of repetition [TR], 2 s; echo time [TE], 30ms; flip angle [FA] 75; field of view [FOV] 192 mm; in-plane resolution, 3.0 × 3.0 mm; 32 slices of 3-mm thickness covering the whole cerebrum) on a 3.0-T magnetic resonance scanner with a standard head coil (Allegra; Siemens, Erlangen, Germany). The interleaved (first slice = bottom) scanning sequence was used. The images were oriented slightly tilted towards the AC-PC line and aligned so that the sample included whole brain. A high-resolutional T1-weighted anatomical brain image of each subject was obtained using an magnetization-prepared rapid gradient-echo sequence (Mugler and Brookeman 1990) with the following parameters: TR = 2500 ms, TE = 4.38 ms, FA = 8°, FOV = 230 × 230 mm^2, resolution = 0.9 × 0.9 mm^2.

Image Processing and Statistical Analysis

Imaging processing and statistical analyses were performed using statistical parametric mapping (SPM99; Wellcome Department of Cognitive Neurology, London, UK) (Friston and others 1995; Worsley and Friston 1995) implemented in Matlab (Mathworks, Sherborn, Massachusetts). The first 8 volumes of each fMRI session were discarded because of unsteady magnetization and the remaining 240 volumes per session (480 volumes per subject) were used for analysis. We initially corrected the differences in slice timing within each volume. To remove the motion artifacts, all volumes were then realigned to the first functional image of each session (Friston and others 1994). After being coregistered with a T1-weighted structural volume, they were normalized in the functional scans to the standard stereotaxic space (Montreal Neurological Institute [MNI] template). Then, the images were spatially smoothed using an isotropic Gaussian kernel with a full-width half maximum of 8 mm. Because the event-related (single-event) design was used in this study, specific effects for Aδ- or C-related sensations were estimated for each subject using a general linear model with a regressor waveform assuming the hemodynamic response (HDR) function beginning at the onset of each laser stimulus. To make statistic inferences at the population level, individual data were then summarized and incorporated into a random-effect model. The threshold was set at $P < 0.001$, uncorrected for multiple comparisons (Friston and others 1998).

Results

Following the stimulation of C nociceptors, the bilateral thalamus, bilateral SII, bilateral middle/anterior insular cortex, bilateral posterior portion of the anterior cingulate cortex (pACC), dorsal parts of the anterior portion of the ACC (aACC), and pre-supplementary motor area (pre-SMA) were significantly activated (Fig. 1a). The HDRs in the bilateral thalamus, bilateral SII, right (ipsilateral) middle insula, and left pACC peaking at 5 or 7 s following stimulation are shown in Figure 1b.

Following Aδ nociceptor stimulation, the bilateral thalamus, bilateral SII, right (ipsilateral) middle insula, and bilateral pACC were significantly activated (Fig. 2a). The HDRs in the bilateral thalamus, bilateral SII, right middle insula, and left pACC peaking at 5 or 7 s following stimulation are shown in Figure 2b. Overall, the time course of HDRs to the activation of C nociceptors was similar with the time resolution of the present fMRI method. The peak of HDRs in these activated regions showed significant differences between Aδ and C nociceptor stimulation. Activity was significantly stronger following the stimulation of Aδ nociceptors than C nociceptors in the right SII ($P < 0.0001$), left SII ($P < 0.05$), right insular ($P < 0.01$), and left pACC ($P < 0.01$) (paired t-test). In contrast, there were no significant differences in the bilateral thalamus ($P = 0.40$ for right thalamus and $P = 0.52$ for left thalamus) (paired t-test).

To identify the activity common to and differing between C and Aδ nociceptor stimulation, we used a conjunction analysis in the SPM analysis (Price and Friston 1997; see also Friston and others [2005] and Nichols and others [2005] for the recent discussion on conjunction analysis). The bilateral SII, bilateral thalamus, right (ipsilateral) middle insula, and bilateral Brodmann's area (BA) 24/32 with the majority of activity occurring in the pACC were activated by both C and Aδ nociceptor stimulation (Table 1 and Fig. 3). We then made a direct comparison between C and Aδ nociceptor stimulation. The activation of the right (ipsilateral) BA32/8/6 including dorsal parts of the aACC and pre-SMA and the bilateral anterior insula was significantly greater following C nociceptor stimulation than Aδ nociceptor stimulation ($P < 0.001$) (Table 2 and Fig. 4). By contrast, there were no regions where activity was significantly stronger following the stimulation of Aδ nociceptors than C nociceptors. The activated regions in ACC and pre-SMA are
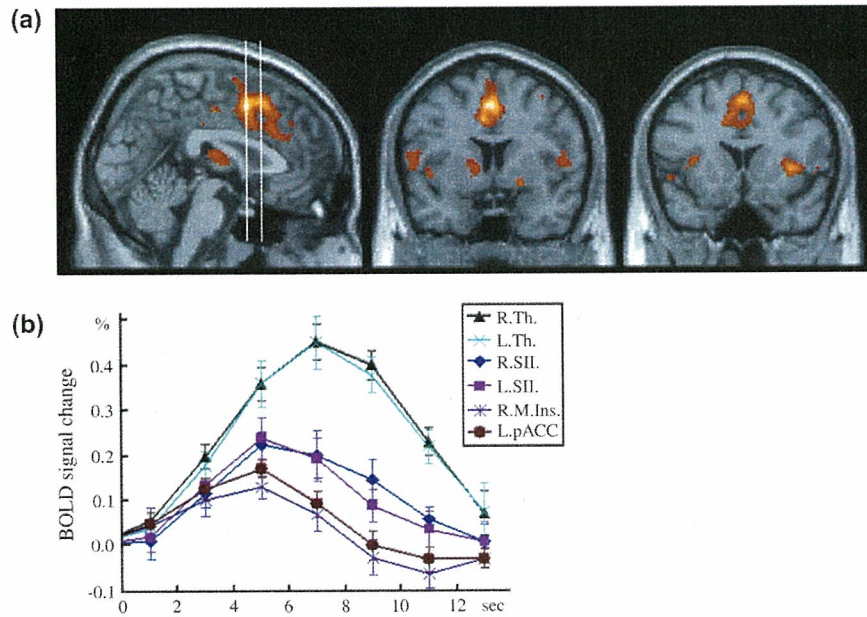
Figure 1. The brain-activated regions and HDRs following C nociceptor stimulation. (a) 1 sagittal (x = 2, left panel) and 2 coronal (y = 6 and 16 for the middle and right panels, respectively) images showing the significant activation to C nociceptor stimulation. Two vertical bars in the left panel indicate the sagittal positions of the 2 coronal planes. (b) Time course of HDRs in the activated regions was illustrated. R. = right (ipsilateral to the stimulation), L. = left (contralateral to the stimulation), M. = middle part, Th. = thalamus, SII = secondary somatosensory cortex, Ins. = insula, pACC = posterior portion of the anterior cingulate cortex. Error bars indicate standard deviation.
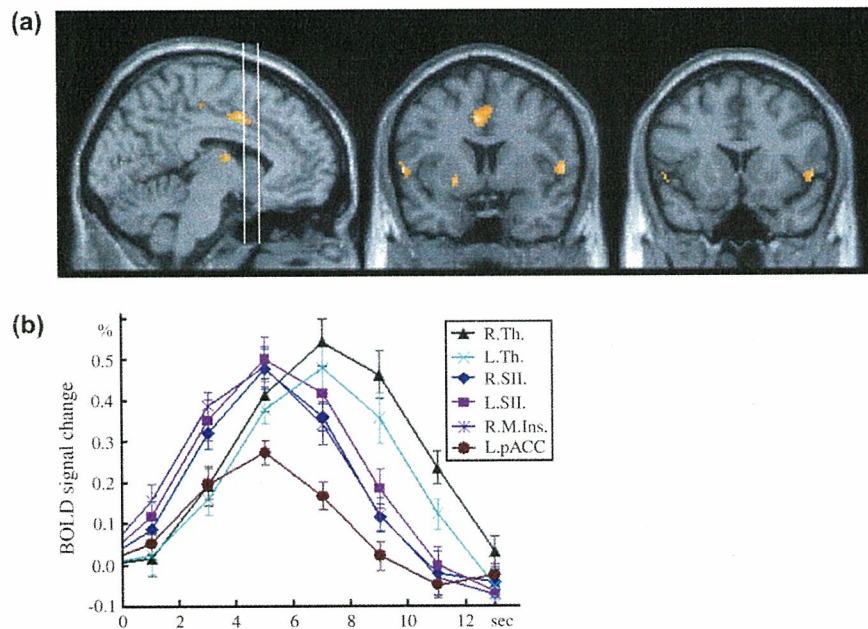

Figure 2. The brain regions activated and HDRs following Aδ nociceptor stimulation. (a) 1 sagittal (x = −6, left panel) and 2 coronal (y = 6 and 16 for the middle and right panels, respectively) images showing the significant activation to Aδ nociceptor stimulation. Two vertical bars in the left panel indicate the sagittal positions of the 2 coronal planes. To make a comparison with Figure 1 easier, the positions of the 2 coronal planes were set identical to those in the previous figure. (b) Time course of HDRs in the activated regions was illustrated. R. = right (ipsilateral to the stimulation), L. = left (contralateral to the stimulation), Th. = thalamus, SII = secondary somatosensory cortex, M. Ins. = middle insula, pACC = posterior portion of the anterior cingulate cortex. Error bars indicate standard deviation.

shown in Figure 5. We used the nomenclature based on Devinsky and others (1995) and Kwan and others (2000) to classify the subregions in the ACC, anterior/posterior and dorsal/ventral portion (Buchel and others 2002).

The time course of HDRs in the 2 regions where C nociceptors were activated more than Aδ nociceptors, the right

(ipsilateral) BA32/8/6 and bilateral anterior insula, is shown in Figure 6. There were differences following Aδ nociceptor stimulation between these 2 regions. Activated Aδ nociceptors in BA32/8/6 were almost absent, indicating that this region was selectively activated following C nociceptor stimulation and is probably related to second pain. The activity was significantly

Table 1

Coordinates (MNI) of regions activated by both C and Aδ nociceptor stimulation

Brain region (side)	x	y	z	Z-score
Thalamus				
Ipsilateral	8	−6	12	4.14
Contralateral	−12	−4	14	4.02
SII				
Ipsilateral	62	−20	18	4.15
Contralateral	−64	−26	18	4.42
Right middle insula				
Ipsilateral	58	4	4	4.12
BA24/32 (pACC)				
Contralateral	−6	4	42	4.02
Ipsilateral	2	10	48	3.73

Table 2

Coordinates (MNI) of specifically activated regions for C nociceptor stimulation

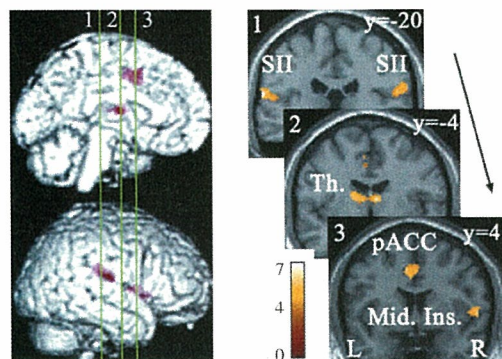| Brain region (side)	x	y	z	Z-score
BA32/8/6				
Midline, Ipsilateral	6	22	50	4.52
Anterior insula				
Ipsilateral	30	21	3	3.91
Contralateral	−31	25	1	3.56

Figure 3. Brain regions commonly activated by C and Aδ nociceptor stimulation. Numbered bars in the left panel indicate locations of coronal slices in the right panel. Activated regions overlaid on an anatomically normalized MRI (MNI template) with their corresponding y coordinates (right side). SII = secondary somatosensory cortex, Th. = thalamus, pACC = posterior portion of the anterior cingulate cortex, Mid. Ins. = middle insula. MNI coordinates in Table 1.
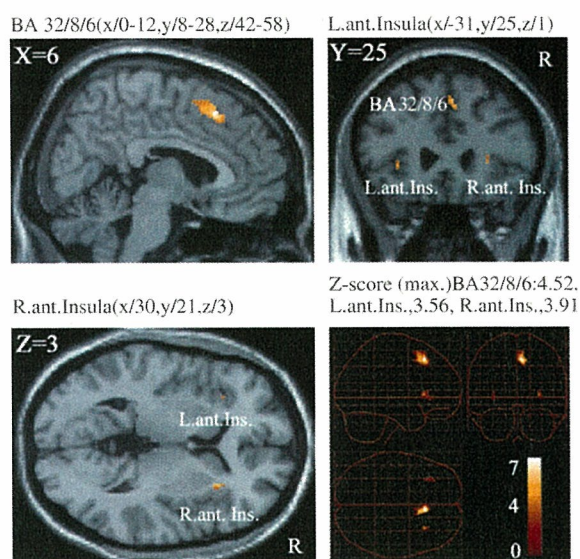

Figure 4. Brain regions differentially activated by C nociceptor stimulation. The activity in these areas was significantly stronger following the stimulation of C nociceptors than Aδ nociceptors ($P < 0.001$, uncorrected) and overlaid on an anatomically normalized MRI (MNI template). BA = Brodmann's area, Ant. Ins. = anterior insula, L. = left, R. = right. MNI coordinates in Table 2.

stronger following the stimulation of C nociceptors than Aδ nociceptors in the time period, 5–9 s, poststimulation ($P < 0.05$) (Fig. 6a). However, the bilateral anterior insula was also activated by Aδ nociceptor stimulation, though to a significantly lesser degree than following C nociceptor stimulation. The HDR peaked at 3 s following Aδ nociceptor stimulation, gradually decreased afterward, and then returned to the baseline level at 6 s. By contrast, HDR peaked at 7 s following C nociceptor stimulation, and a significant difference was found between the 2 stimulus conditions at 5 and 7 s poststimulation ($P < 0.05$) (Fig. 6b). Therefore, this region is considered to be important for both C and Aδ nociceptor stimulation but is more specifically activated by C nociceptor stimulation, probably related to second pain.

Discussion

In the present fMRI study, we found that the activity in the right (ipsilateral) BA32/8/6, including the dorsal parts of the aACC and pre-SMA, and the bilateral anterior insula was significantly stronger following the stimulation of C nociceptors than Aδ nociceptors, though several regions were activated by both stimuli.

This is the first neuroimaging study to use the phasic stimulation of C nociceptors. As a method for the tonic stimulation of C nociceptors, the injection of capsaicin is commonly used, and a few studies using PET (Andersson and

others 1997; Iadarola and others 1998; May and others 1998) and fMRI (Baron and others 1999) reported that the thalamus, striatum, SI, SII, insula cortex, cingulate cortex, prefrontal cortex, and SMA were activated in normal healthy subjects. Activity in the insular cortex was also identified by fMRI following touch stimulation of C fiber tactile afferents in a unique patient lacking large myelinated afferents (Olausson and others 2002). In the present study, the bilateral thalamus, bilateral SII, bilateral middle/anterior insula, bilateral ACC, and pre-SMA were activated, consistent with previous studies using capsaicin-induced pain. By contrast, no activation of the SI or prefrontal cortex was found. Because capsaicin-induced pain is a tonic pain reflecting a mixture of bottom–up and top–down processes and complex pain-coping strategies, the difference in regions activated obtained with the capsaicin injection and our method was probably caused by the difference in the method of stimulation used. However, the finding that the activity in the right (ipsilateral) BA32/8/6, including the dorsal parts of the aACC and pre-SMA, and the bilateral anterior insula, particularly the former, was significantly stronger following stimulation of C nociceptors than Aδ nociceptors was novel.

Following the stimulation of Aδ nociceptors in the present study, the bilateral thalamus, bilateral SII, right (ipsilateral) middle insula, and pACC were activated, consistent with recent neuroimaging studies using PET and fMRI following stimulation with CO_2 or a Tm:YAG laser. However, a German group (Bingel

● Common activated area for C & Aδ
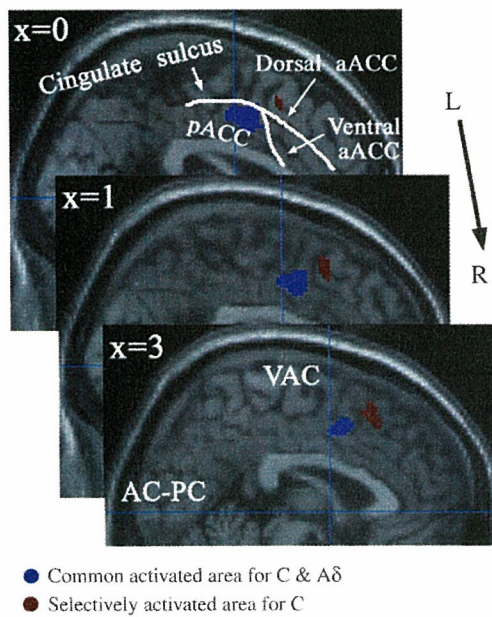● Selectively activated area for C

Figure 5. Activations in the ACC and pre-SMA overlaid on an anatomically normalized MRI (MNI template). These are shown from left (top part of the image) to right (bottom part of the image) with their corresponding MNI template x coordinates. The blue vertical line indicates the line through the anterior commissure (VAC). aACC = anterior portion of the anterior cingulate cortex, pACC = posterior portion of the anterior cingulate cortex.

and others 2002; Bornhovd and others 2002; Buchel and others 2002; Bingel, Glascher, and others 2004; Bingel, Lorenz, and others 2004) reported that many regions involving the SI, hippocampus, amygdala, prefrontal cortex, SMA, motor cortex, putamen, red nucleus, brainstem, and cerebellum were also activated in addition to the regions identified in the present study. We consider the difference between their findings and ours to be mainly due to the method of analysis because the German group used a fix-effect model whereas we used a random-effect model during the group analysis with un-corrected values and set the threshold at $P < 0.001$. In any case, the areas important for pain perception may be those where both groups identified activity.

· We found activity in the pACC following the stimulation of both Aδ and C nociceptors and in the dorsal part of the aACC following the stimulation of only C nociceptors. Hutchison and others (1999) detected activity in the pACC following painful thermal stimulation using single-neuron recordings in conscious subjects. Buchel and others (2002) demonstrated that the pACC is associated with pain intensity, and dorsal parts of the aACC are associated with cognitive processing like attention and working memory and stimulus awareness related to pain. In addition, the dorsal ACC also plays important roles in cognition, motor control, and emotional processing (Bush and others 2002). Therefore, our findings indicate that the activation of the dorsal parts of the aACC through the stimulation of C nociceptors, probably related to second pain, is closely related to the cognitive aspect of pain as compared with the stimulation of the Aδ nociceptors (first pain). Recently, Bush and others (2000) and Vogt and others (2003) reviewed anatomical and physiological findings of cingulate cortex. Bush and others (2000) separated ACC into 2 parts by their roles; the more
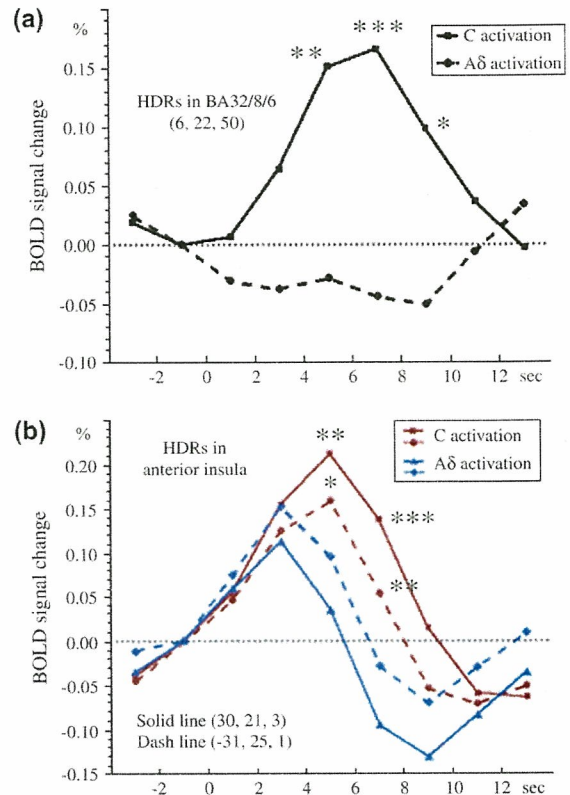
Figure 6. Time course of the HDRs in the BA32/8/6 and bilateral anterior insula following stimulation of C and Aδ nociceptors. (a) In the right (ipsilateral) BA32/8/6, the HDR following Aδ nociceptor stimulation was almost below the baseline, whereas that following C nociceptor stimulation was very large. The difference between them, 5–9 s, after stimulation was significant. (b) In the bilateral anterior insula cortex (solid/dashed line = right/left anterior insula), the HDR following Aδ nociceptor stimulation peaked at 3 s, rapidly decreased thereafter, and had returned to the baseline level at 6 s. By contrast, the HDR following C nociceptor stimulation was large for a long period, peaking at 5 s, and the difference between 5 and 7 s after stimulation was significant (the paired t-test was calculated from red solid to blue solid lines and red dashed to blue dashed lines) (*$P < 0.05$, **$P < 0.01$, ***$P < 0.001$).

anterior part plays a main role for emotional tasks and the posterior part does so for tasks. The activated region found in the present study was consistent with the emotional region reported by them; Vogt and others (2003) also separated the cingulate cortex into 3 parts: noxious thermal region, emotional region, and nonemotional region, and the activated region found in the present study was consistent with the noxious re-gion and emotional region reported by them, mainly the former.

Activation in the SMA has been reported following various noxious stimulations such as heat (Coghill and others 1994; Kwan and others 2000), cooling (Kwan and others 2000), CO_2 laser (Svensson and others 1997), ethanol injection (Hsieh and others 1996), and thermal grill (Craig and others 1996). Kwan and others (2000) reported fMRI study of the activation of the ACC and surrounding medial wall using innocuous and noxious thermal-related stimuli and motor-related stimuli and noxious stimuli activated mainly aACC, pACC, and SMA proper and modestly pre-SMA too. Picard and Strick (2001) reviewed imaging studies of the premotor cortex and concluded that it might be more appropriate to consider the pre-SMA as a functional component of the prefrontal cortex rather than

as a premotor area. Because the dorsal parts of the aACC is also considered as a cognitive region (Bush and others 2002), it seems appropriate that both pre-SMA and caudal division of ACC play a main role for cognitive function for second pain perception.

Studies of lesions in animals and humans, functional imaging related to attention and emotion, and opioid-binding experiments have shown that the anterior insula is coactivated with the ACC to reflect active modulation by the affective agent of pain perception (Peyron and others 2000; Schnizler and Ploner 2000; Craig 2002). Our finding that the activity in the bilateral anterior insular cortex was significantly stronger following the stimulation of C nociceptors than Aδ nociceptors, which is probably related to second pain, reflects greater attention and behavioral motivation as compared with first pain (Aδ nociceptor stimulation).

It is obvious that first pain and second pain are experienced differently probably because of several anatomical and physiological differences. In the dorsal horn of the spinal cord, lamina II is the input nucleus for C nociceptors and laminae I and V are major output nuclei for Aδ nociceptors (Willis 1985). Since Melzack and Casey (1968) divided the nociceptive system into lateral (sensory-discriminative aspects of pain) and medial (affective-motivational aspects of pain) systems, the supraspinal parts of the nociceptive system have been investigated by a large number of functional imaging studies (see review by Treede and others 1999). However, the difference of activated brain regions between Aδ and C nociceptor stimulation remained to be investigated. We found that the activity in the bilateral insula and dorsal parts of the ACC and pre-SMA was significantly greater following stimulation of C nociceptors than Aδ nociceptors in this study. These findings may indicate that the C nociceptors play a more important role in the medial system, whereas the Aδ nociceptors play a more important role in the lateral system, the sensory–discriminative aspects of pain.

In conclusion, our findings seem to suggest that the differences in brain activity between first and second pain perception probably reflect distinct biological functions of the 2 sensations as found in this study. It is considered that first pain aims at achieving relative safety from the source of injury, whereas second pain, with its strong affective component, attracts longer lasting attention and initiates behavioral responses to limit further injury and optimize recovery (Wall 1979). Therefore, dorsal parts of the aACC, pre-SMA, and anterior insular cortex should play some role in the perception of second pain.

Notes

References

Andersson JL, Lilja A, Hartvig P, Langstrom B, Gordh T, Handwerker H, Torebjork E. 1997. Somatotopic organization along the central sulcus, for pain localization in humans, as revealed by positron emission tomography. Exp Brain Res 117:192-199.

Baron R, Baron Y, Disbrow E, Roberts TP. 1999. Brain processing of capsaicin-induced secondary hyperalgesia: a functional MRI study. Neurology 11:548-557.

Bingel U, Glascher J, Weiller C, Buchel C. 2004. Somatotopic representation of nociceptive information in the putamen: an event-related fMRI study. Cereb Cortex 14:1340-1345.

Bingel U, Lorenz J, Glauche V, Knab R, Glascher J, Weiller C, Buchel C. 2004. Somatotopic organization of human somatosensory cortices for pain: a single trial fMRI study. Neuroimage 23:224-232.

Bingel U, Quante M, Knab R, Bromm B, Weiller C, Buchel C. 2002. Subcortical structures involved in pain processing: evidence from single-trial fMRI. Pain 99:313-321.

Bornhovd K, Quante M, Glauche V, Bromm B, Weiller C, Buchel C. 2002. Painful stimuli evoke different stimulus-response functions in the amygdala, prefrontal, insula and somatosensory cortex: a single-trial fMRI study. Brain 125:1326-1336.

Bragard D, Chen CAN, Plaghki L. 1996. Direct isolation of ultra-late (C-fibre) evoked brain potentials by CO$_2$ laser stimulation of tiny cutaneous surface areas in man. Neurosci Lett 209:81-84.

Bromm B, Treede RD. 1984. Nerve fibre discharges, cerebral potentials and sensations induced by CO$_2$ laser stimulation. Hum Neurobiol 3:33-40.

Buchel C, Bornhovd K, Quante M, Glauche V, Bromm B, Weiller C. 2002. Dissociable neural responses related to pain intensity, stimulus intensity, and stimulus awareness within the anterior cingulate cortex: a parametric single-trial laser functional magnetic resonance imaging study. J Neurosci 22:970-976.

Bush G, Luu P, Posner MI. 2000. Cognitive and emotional influences in anterior cingulate cortex. Trends Cogn Sci 4:215-222.

Bush G, Vogt BA, Holmes J, Dale AM, Greve D, Jenike MA, Rosen BR. 2002. Dorsal anterior cingulate cortex: a role in reward-based decision making. Proc Natl Acad Sci USA 99:523-528.

Coghill RC, Talbot JD, Evans AC, Meyer E, Gjedde A, Bushnell MC, Duncan GH. 1994. Distributed processing of pain and vibration by the human brain. J Neurosci 14:4095-4108.

Craig AD. 2002. How do you feel? Interoception: the sense of the physiological condition of the body. Nat Rev Neurosci 3:655-666.

Craig AD, Reiman EM, Evans A, Bushnell MC. 1996. Functional imaging of an illusion of pain. Nature 384:258-260.

Devinsky O, Morrell MJ, Vogt BA. 1995. Contributions of anterior cingulate cortex to behaviour. Brain 118:279-306.

Friston KJ, Fletcher P, Josephs O, Holmes A, Rugg MD, Turner R. 1998. Event-related fMRI: characterizing differential responses. Neuroimage 7:30-40.

Friston KJ, Holmes AP, Poline JB, Grasby PJ, Williams SC, Frackowiak RS, Turner R. 1995. Analysis of fMRI time-series revisited. Neuroimage 1:45-53.

Friston KJ, Holmes AP, Worsley KJ, Poline JP, Frith, CD, Frackowiak RSJ. 1994. Statistical parametric maps in functional imaging: a general linear approach. Hum Brain Mapp 2:189-210.

Friston KJ, Penny WD, Glaser DE. 2005. Conjunction revisited. Neuroimage 25:661-667.

Holzer P. 1991. Capsaicin: cellular targets, mechanisms of action, and selectivity for thin sensory neurons. Pharmacol Rev 43:143-201.

Hsieh J-C, Ståhle-Bäckdahl M, Hägermark O, Stone-Elander S, Rosenquist G, Ingvar M. 1996. Traumatic nociceptive pain activates the hypothalamus and the periaqueductal gray: a positron emission tomography study. Pain 64:303-314.

Hutchison WD, Davis KD, Lozano AM, Tasker RR, Dostrovsky JO. 1999. Pain-related neurons in the human cingulate cortex. Nat Neurosci 2:403-405.

Iadarola MJ, Berman KF, Zeffiro TA, Byas-Smith MG, Gracely RH, Max MB, Bennett GJ. 1998. Neural activation during acute capsaicin-evoked pain and allodynia assessed with PET. Brain 121:931-947.

Kakigi R, Tran TD, Qiu Y, Wang X, Nguyen TB, Inui K, Watanabe S, Hoshiyama M. 2003. Cerebral responses following stimulation of unmyelinated C-fibers in humans: Electro- and magneto-encephalographic study. Neurosci Res 45:255-275.

Kwan CL, Crawley AP, Mikulis DJ, Davis KD. 2000. An fMRI study of the anterior cingulate cortex and surrounding medial wall activations evoked by noxious cutaneous heat and cold stimuli. Pain 85:359-374.

Mauguiere F, Frot M, Peyron R, Garcia-Larrea L, Laurent B, Michel D. 1999. The role of parietal opercular and insular cortex in pain sensation in humans: data from PET activation studies and intra-cortical recordings of CO$_2$ laser evoked potentials (LEPs). Electroencephalogr Clin Neurophysiol Suppl 49:255-260.

May A, Kaube H, Buchel C, Eichten C, Rijntjes M, Juptner M, Weiller C, Diener HC. 1998. Experimental cranial pain elicited by capsaicin: a PET study. Pain 74:61-66.

Melzack R, Casey KL. 1968. Sensory, motivational, and central control determinations of pain. A new conceptional model. In: Kenshalo DR, editor. The Skin Senses. Springfield, IL: Charles C. Thomas. p 423-443.

Mendell LM, Wall PD. 1965. Responses of single dorsal cord cells to peripheral cutaneous unmyelinated fibres. Nature 3:97-99.

Mor J, Carmon A. 1975. Laser emitted radiant heat for pain research. Pain 1:233-237.

Mugler JP, Brookeman JR. 1990. Three-dimensional magnetization-prepared rapid gradient-echo imaging (3D MP RAGE). Magn Reson Med 15:152-157.

Nichols T, Brett M, Andersson J, Wager T, Poline JB. 2005. Valid conjunction inference with the minimum statistic. Neuroimage 25:653-660.

Ochoa J, Torebjork E. 1989. Sensations evoked by intraneural microstimulation of C nociceptor fibres in human skin nerves. J Physiol 415:583-599.

Olausson H, Lamarre Y, Backlund H, Morin C, Wallin BG, Starck G, Ekholm S, Strigo I, Worsley K, Vallbo AB, Bushnell MC. 2002. Unmyelinated tactile afferents signal touch and project to insular cortex. Nat Neurosci 9:900-904.

Opsommer E, Masquelier E, Plaghki L. 1999. Determination of nerve conduction velocity of C-fibers in humans from thermal thresholds to contact heat (thermode) and from evoked brain potentials to radiant heat (CO$_2$ laser). Neurophysiol Clin 29:411-422.

Peyron R, Laurent B, Garcia-Larrea L. 2000. Functional imaging of brain responses to pain. A review and meta-analysis. Neurophysiol Clin 30:263-288.

Picard N, Strick PL. 2001. Imaging the premotor areas. Curr Opin Neurobiol 11:663-672.

Plaghki L, Mouraux A. 2003. How do we selectively activate skin nociceptors with a high power infrared laser? Physiology and biophysics of laser stimulation. Neurophysiol Clin 33:269-277.

Ploner M, Gross J, Timmermann L, Schnitzler A. 2002. Cortical representation of first and second pain sensation in humans. Proc Natl Acad Sci USA 17:12444-12448.

Price CJ, Friston KJ. 1997. Cognitive conjunction: a new approach to brain activation experiments. Neuroimage 5:261-270.

Price DD, Hu JW, Dubner R, Gracely RH. 1977. Peripheral suppression of first pain and central summation of second pain evoked by noxious heat pulses. Pain 3:57-68.

Qiu Y, Fu Q, Wang X, Tran TD, Inui K, Iwase S, Kakigi R. 2003. Microneurographic study of C fiber discharges induced by CO$_2$ laser stimulation in humans. Neurosci Lett 15:25-28.

Qiu Y, Inui K, Wang X, Nguyen BT, Tran TD, Kakigi R. 2004. Effects of distraction on magnetoencephalographic responses ascending through C-fibers in humans. Clin Neurophysiol 115:636-646.

Qiu Y, Inui K, Wang X, Tran TD, Kakigi R. 2001. Conduction velocity of the spinothalamic tract in humans as assessed by CO$_2$ laser stimulation of C-fibers. Neurosci Lett 311:181-184.

Qiu Y, Inui K, Wang X, Tran TD, Kakigi R. 2002. Effects of attention, distraction and sleep on CO$_2$ laser evoked potentials related to C-fibers in human. Clin Neurophysiol 113:1579-1585.

Sawamoto N, Honda M, Okada T, Hanakawa T, Kanda M, Fukuyama H, Konishi J, Shibasaki H. 2000. Expectation of pain enhances responses to nonpainful somatosensory stimulation in the anterior cingulate cortex and parietal operculum/posterior insula: an event-related functional magnetic resonance imaging study. J Neurosci 20:7438-7445.

Schmidt RF, Schaible HG, Messlinger K, Heppelmann B, Hanesch U, Pawlak M. 1994. Silent and active nociceptors: structure, functions, and clinical implications. In: Gebhart GF, Hammond DL, Jensen TS, editors. Proceedings of the 7th World Congress on Pain. Seattle, WA: IASP Press. p 213-250.

Schnitzler A, Ploner M. 2000. Neurophysiology and functional neuroanatomy of pain perception. J Clin Neurophysiol 17:592-603.

Svensson P, Minoshima S, Beydoun A, Morrow TJ, Casey KL. 1997. Cerebral processing of acute skin and muscle pain in humans. J Neurophysiol 78:450-460.

Szallasi A. 1994. The vanilloid (capsaicin) receptor: receptor types and species differences. Gen Pharmacol 25:223-243.

Tran TD, Inui K, Hoshiyama M, Lam K, Kakigi R. 2003. Conduction velocity of the spinothalamic tract following CO$_2$ laser stimulation of C-fiber in humans. Pain 95:125-131.

Tran TD, Inui K, Hoshiyama M, Lam K, Qiu Y, Kakigi R. 2002. Cerebral activation by the signals ascending through unmyelinated C-fibers in humans: a magnetoencephalographic study. Neuroscience 113:375-386.

Tran TD, Lam K, Hoshiyama M, Kakigi R. 2001. A new method for measuring the conduction velocities of Aβ-, Aδ- and C-fibers following electric and CO$_2$ laser stimulation in humans. Neurosci Lett 301:187-190.

Treede RD, Kenshalo DR, Gracely RH, Jones AK. 1999. The cortical representation of pain. Pain 79:105-111.

Treede RD, Meyer RA, Lesser RP. 1994. Similarity of threshold temperatures for first pain sensation, laser-evoked potentials, and nociceptor activation. In: Gebhart GF, Hammond DL, Jensen TS, editors. Proceedings of the 7th World Congress on Pain. Seattle, WA: IASP Press. p 857-865.

Vogt BA, Berger GR, Derbyshire SWG. 2003. Structural and functional dichotomy of human midcingulate cortex. Eur J Neurosci 18:3134-3144.

Wall PD. 1979. On the relation of injury to pain. The John J. Bonica lecture. Pain 6:253-264.

Willis WD. 1985. The Pain System. Basel, Switzerland: Karger.

Worsley KJ, Friston, KJ. 1995. Analysis of fMRI time-series revisited—again. Neuroimage 2:173-181.

Xu X, Fukuyama H, Yazawa S, Mima T, Hanakawa T, Magata Y, Kanda M, Fujiwara N, Shindo K, Nagamine T, Shibasaki H. 1997. Functional localization of pain perception in the human brain studied by PET. Neuroreport 8:555-559.

感覚情報処理（1）

感覚情報の階層的処理
Hierarchical processing of sensory information

乾　幸二　　柿木　隆介*
INUI Koji　　KAKIGI Ryusuke

　脳磁図を用いて触覚，痛覚，視覚および聴覚情報処理について検討し，以下のような共通点を見い出した．
1）感覚情報は基本的に隣接する領野へ約5ミリ秒の潜時で順次伝えられ，その結果一定方向へ向かう処理の流れを形成する．
2）並行する複数の処理経路がある．
3）初期活動はすべて活動の向きを約10ミリ秒間隔で逆転させ，共通する層内伝導様式を示唆する．
　以上の知見は動物での階層性研究と合致し，ヒトでの階層的処理を支持する．

はじめに

　感覚情報の階層的処理仮説は，1950年代にHubel と Wiesel によって提唱され，成功を収めた．彼らは視覚野の細胞の受容野が段階的に複雑化することを見い出し，それぞれの階層の興奮がそれより早い階層の複数の活動に依存していると考えた[1]．その後の解剖学的研究はこのような階層的処理を支持し，さらに視覚以外の感覚系でも同様の階層構造があると考えられるようになった．しかし，主な研究手法が受容野と解剖学的連絡であるためヒトでの知見は乏しく，階層的処理仮説がヒト感覚情報処理にもあてはまるかどうかについては十分な情報が得られていない．本稿ではまず階層処理仮説を支持する動物実験での知見を概説し，その後脳磁図を用いて行ったわれわれの研究結果を紹介する．

階層的処理を支持する知見

1. 解剖学的連絡

　一般に大脳皮質のⅢ層にある細胞の軸索は，隣接する領野のⅣ層に投射する．この皮質結合パターンは情報が順次伝えられる（feedforward projection）と考えられる連絡に共通してみられ，例えば視覚野では，V1からV2へ，V2からV4へ，V4からTE（inferotemporal）への連絡にこの結合パターンがみられる[2]．逆にV4からV2へ，V2からV1へと情報処理の起始点に向かって戻る方向の連絡や（feedback projection），同一階層間の横の連絡（lateral projection）では全く異なる皮

質－皮質結合パターンがみられる．したがって，Ⅲ層出力－Ⅳ層入力の結合パターンは，その連絡がfeedforwardであることを示唆する．上記視覚野の連絡パターンは，V1-V2-V4-TEの順に情報が伝達されることを予想させ，17野，18野，19野の順に視覚細胞の受容野が段階的に複雑化するとのHubelとWieselの報告とも合致する．このような皮質間連絡の結合パターンは視覚野以外の領野でも認められ，各感覚系の解剖学的階層構造がFellemanとVan Essenによってまとめられている[3]．皮質間連絡の結合パターンのほかに，組織学的所見からある領野の階層連鎖の中での位置を類推する方法がある．たとえば体性感覚野では，3b野が典型的な投射野の特徴を示すのに対し，1野，2野，5野と後方へ進むにつれて連合野としての色彩が強くなる．さらに，acetylcholinesteraseやcytochrome oxidaseのように階層によって一定の傾向に従って分布が変化する物質があり，解剖学的階層構造を知るうえで重要な知見の一つとなっている．これらの研究手法はヒトの組織にも適用することができ，動物と同様の知見が得られている．

2．受容野

初期のHubelらの研究ですでに明らかにされたように，一般に細胞の受容野は階層が上位になるほど大きく，複雑になる．このような所見は，ある階層の細胞の活動がそれより下位の階層の複数の情報に依存していることを示し，階層的処理を支持する．当然のことながら受容野の複雑化には重要な意味があり，いかにして最小単位で受容された感覚情報が一定のまとまった感覚情報に洗練されていくか，という機能的活動様式獲得過程が詳細な受容野研究によって明らかにされてきた．たとえば覚醒サルを用いて体性感覚野の細胞の受容野を緻密に検討してきた岩村ら[4]の報告によれば，3野の細胞がほぼ指の一分節に相当する受容野を持つのに対し，1野あるいは2野では受容野は大きく，多指にわたるものが観察され，さらに5野では両側の受容野を示す細胞がみられるよ

うになる（3野－1野－2野－5野の階層連鎖）．1指に興奮性，2-5指の広い範囲に抑制性の受容野を持つ2野の細胞を例にとると，3野の細胞の受容野がほぼ1分節に限られることを考えると，この細胞は相当数の細胞からの情報を受け取っていると考えられる．さらに，このような細胞は小さなものをつまんだときに興奮し，大きなものを手のひら全体で握ったときには抑制されるのであり，特定の状況に特化した細胞であると想像される．3野のみならず1野，2野でも完全な体部位再現がある（多重再現）との報告があるが[5]，階層が高くなるにつれて，受容野の局在よりもむしろこのような特定の興奮パターンが重視されていく，と考えるのが妥当と思われる．このように階層を進むにつれて細胞の受容野は機能的な意味を獲得していくのであり，一連の岩村らの研究は体性感覚系の階層処理構造を明らかにしたのみならず，階層処理の意義を受容野の面から見事に示したと言える．

3．破壊実験

感覚情報が階層的に処理されるとすれば，ある階層の破壊がもたらす効果は，その階層のレベルによって異なるはずである．最も下位の階層を破壊すればそれ以降の処理がすべて失われ，高い階層の破壊ではその階層を経由しない処理はすべて保たれることになる．単一細胞の応答性の研究では，マカク第一次体性感覚野（S1）を破壊すると第二次体性感覚野（S2）の細胞の応答性は消失する，聴覚野のcore領野（第1階層）の破壊はbelt領野（第2階層）の応答性を消失させる，V1の破壊はV2の応答性を消失させる，などの報告がある．いずれも，第2階層の活動が第1階層に依存していることを示す結果である．

細胞の単純な応答性をみるのではなく破壊がもたらす機能的変化を調べる研究もあり，たとえば視覚野では，V1の破壊は破壊部位のretinotopyに一致した視野の暗点を生じるのに対し，頭頂葉へ向かう背側経路の破壊は空間認知の選択的障害，腹側経路の破壊は形体認知の選択的障害を生じ，

V1を起始点とする複数の並列階層が推定される[6]．ヒトでは脳血管障害などの理由により脳の一部に損傷を受けた患者の機能的変化が同様に検討され，概ね動物実験と合致する階層性が類推できる．たとえば，運動視に関与すると考えられる両側V5野に損傷のある患者の報告では，基本的な視覚認知は保たれているにもかかわらず動きがわからないという．この症例から，V5が最下層（V1）よりも高い位置にあり，かつ基本的な物体認知とは別の階層連鎖にあることが類推できる．

4．活動のタイミング

感覚情報の階層処理は，階層が高くなるにつれて活動潜時が長くなることを予想させる．1野の活動が3b野に依存しているなら，連絡に要する時間分だけ1野の活動潜時は3b野よりも遅れるであろうと考える単純な理屈である．単一細胞記録の手法によりこのようなデータは容易に得られるように思われるが，実際には各領野の活動潜時を比較する目的には単一細胞記録は不向きであり，領野間での階層性を活動タイミングの面から明瞭に示した研究はほとんどみあたらない．これは，大脳皮質には反応特性の異なる種々の細胞が混在しているためで，ある皮質部位の細胞を応答潜時から明瞭なクラスターに分離するには相当数の記録が必要となる．たとえば，フラッシュ刺激に応答するマカクV1細胞の応答潜時は概ね20～100msと幅広く，少ないサンプルでV1とV2で潜時を比較するのは不適切である．フィールド電位の記録は活動タイミングを知るうえでは単一細胞記録より優れている．フィールド電位は時間的空間的に類似した活動の総和を記録するためで，特に最も早い潜時の活動の決定には優れている．

しかし，大脳皮質各層の活動が混在して記録される欠点は単一細胞記録と同様であり，この欠点を補うために電流源密度推定法（CSD）[7]という手法が用いられることもある．ヒトで記録可能な脳波や脳磁図は基本的にフィールド電位と同じものを記録するため，ヒトと動物のデータを比較するうえでもCSD研究は重要である．しかし，動物実験でのフィールド電位記録には幅広い領野からの同時記録が困難という限界があり，階層連鎖の仮説にあう活動タイミングの証明は不十分である．ヒトでは実験手法の制限から，活動タイミングの詳細はほとんど知られていない．

脳磁図を用いたヒト感覚野の階層性研究

われわれの研究室では，脳磁図を用いた活動タイミングの検討により各種感覚系の情報処理階層性を研究してきたのでその結果を紹介し[8]−[12]，動物のデータとの比較を若干加える．データはすべてBTi社製の脳磁計を用いて記録したもので，オーバーラップする複数の皮質活動を分離するために多信号源解析法を用いている．刺激は，触覚が左手背への電気刺激，聴覚が左耳へのクリック音刺激，視覚が左眼へのフラッシュ刺激，痛覚が左手背への表皮内電気刺激である．単一被験者からのデータの解析例を図1に，それぞれの感覚系の主な領野の活動時間経過（全被験者平均波形）を図2に示す．

1．情報処理の流れ

ある領野の活動は基本的に近接する領野へ伝えられ，その結果一定方向の処理の流れを形成する．触覚では最初の皮質活動はS1の3b野にあり，その後1野，2野，5野と中心後回を後方へ伝えられていく．聴覚ではHeschl回内側部にある第一次聴覚野（A1あるいはcore）から，Heschl回外側部（belt），ついで上側頭回（parabelt）へと進み，側頭葉平面を外側へ進む流れとなる．視覚ではV1からV2，さらにV4へと後頭葉後部から始まり側頭葉へと進む経路を形成する．このような情報処理様式は処理スピードの観点からきわめて合理的である．これらの結果は階層的処理の概念に合致するのみならず，現在動物実験でのデータを基に考えられている階層構造ともきわめてよく一致する．